HOKKAIDO UNIVERSITY

Title	Approaches for a probabilistic evaluation in predictive microbiology : Interpretation of stochastic bacterial inactivation process in a population and single cell level
Author(s)	小山, 健斗
Degree Grantor	北海道大学
Degree Name	博士(農学)
Dissertation Number	甲第13582号
Issue Date	2019-03-25
DOI	https://doi.org/10.14943/doctoral.k13582
Doc URL	https://hdl.handle.net/2115/73924
Type	doctoral thesis
File Information	Kento_Koyama.pdf

Hokkaido University Collection of Scholarly and Academic Papers : HUSCAP

Approaches for a probabilistic evaluation in predictive microbiology: Interpretation of stochastic bacterial inactivation process in a population and single cell level

（予測微生物学における確率的評価のためのアプローチ：
集団および単一細胞レベルにおける確率的細菌不活化プロセスの解釈）

Hokkaido University
Graduate School of Agriculture
Division of Biosystems Sustainability
Doctor Studies

Kento Koyama

Acknowledgements

I would like to thank Dr. Shigenobu Koseki, my supervisor, for his excellent guidance and encouragement over the past five years. This research has been a great experience for me. I would also like to thank Dr. Shuso Kawamura for his advice regarding both this research and my future career, which has been extremely helpful. Warm thanks are also due to Professor Kostas Koutsoumanis, of Aristotle University of Thessaloniki, who accepted me as a visiting Ph.D. student from October 1, 2017, to the end of February 2019. I had a very nice time working together there. During the course of my Ph.D., I worked with several students, including Zafiro Aspridou at Aristotle University of Thessaloniki and Hiroki Abe, Kohei Takeoka, Natsuki Tsuruma, and Satoko Hiura at Hokkaido University. I thank them for their perseverance through the research.

This work was supported by JSPS KAKENHI Grants-in-Aid for JSPS Fellows [grant number 17J04163], JSPS Overseas Challenge Program for Young Researchers, and Nitobe School Advanced Program 2017.

Finally, I want to say thank you to all of the laboratory workers in Japan and Greece who made my time in the office such a pleasant experience.

Table of Contents

Page

Acknowledgements ····· **i**

Table of Contents ····· **ii**

List of Tables ····· **iii**

List of Figures ····· **iv**

Chapter 1 General Introduction ····· **1**

1.1. Current microbial food safety ····· 1

1.2. International food safety framework ····· 2

1.3. Traditional predictive microbiology ····· 2

1.4. Problems with traditional predictive microbiology ····· 3

1.5. Variability associated with predictive microbiology ····· 4

1.6. Objective of this study ····· 5

Chapter 2 Computer Simulation of Inactivation of Bacterial Populations ····· **6**

2.1. Introduction ····· 6

2.2. Materials and methods ····· 6

2.2.1. Mathematical-based assumptions ····· 6

2.2.2. Procedure for computer simulation of bacterial inactivation ····· 8

2.2.3. Trend of time-to-inactivation of bacterial population ····· 9

2.2.4. Death probability in the bacterial population ····· 11

2.2.5. Validation of bacterial inactivation behavior in the bacterial population ··· 12

2.3. Results ····· 13

2.4. Discussion ····· 21

Chapter 3 Mathematical Modeling of Inactivation ····· **24**

3.1. Introduction ····· 24

3.2. Material and methods ····· 25

3.2.1. Stochastic calculation of the time required for a specific decrease in the number of cells ····· 25

3.2.2. Stochastic calculation for changing the number of survivors ····· 30

3.3. Results and Discussion ····· 35

Chapter 4 Summary ····· **42**

References ····· **44**

List of Tables

Page

Table

2-1. Rate parameter b and shape parameters n of Weibull distribution in inactivation kinetics ($log_{10}N(t) = -bt^n + log_{10}N_0$) discussed in this work ····· 10

3-1. Comparison of probability of a population containing survivors between inactivation kinetic calculation (Eq. (3-12)) and stochastic calculation with variability in individual cell inactivation time and initial cell number (Eq. (3-11)) ····· 35

List of Figures

Figure

Page

2-1. Linear (A), downward concavity (B), and upward concavity (C) log-Weibull models with $N_0 = 10^9$ initial cells. ····· 10

2-2. Death probability estimation using inactivation kinetics model ($N_0 = 10^3, b = 1.35, n = 0.5$). The points $P = 0.9$ (90% probability of death), 0.99, 0.999, 0.9999, and 0.99999 are indicated by a square, circle, triangle, plus, and cross, respectively. ····· 12

2-3. (Top row) Monte Carlo simulation results (100 simulations) for the linear (A), downward concavity (B), and upward concavity (C) inactivation curve with $N_0 = 10^5$ initial cells. (Bottom row) Histograms showing time-to-inactivation of bacterial population for the linear (D), downward concavity (E), and upward concavity (F) inactivation curves. ·· 14

2-4. (Top row) Monte Carlo simulation results (100 simulations) for the linear ($b = 0.2, n = 1$) (A), downward concavity ($b = 0.005, n = 2$) (B), and upward concavity ($b = 1, n = 0.5$) (C) inactivation curves with $N_0 = 10, 10^3, 10^5$ initial cells. (Bottom row) Histograms showing time-to-inactivation of bacterial population for the linear (D), downward concavity (E), and upward concavity (F) inactivation curves. ····· 15

2-5. Variance of time-to-inactivation of bacterial population (100 simulations) with various numbers of initial cells for log-linear (A), downward concavity (B), and upward concavity (C) cases. The low, middle, and high inactivation rates of the kinetics are indicated by a square, circle, and triangle, respectively. ····· 16

2-6. Representation of the death probability of bacterial population for log-linear ($b = 0.2, n = 1$) (A), downward concavity ($b = 0.005, n = 2$) (B), and upward concavity ($b = 1.35, n = 0.5$) (C) cases calculated via our stochastic approach. The interfaces $P = 0.9$ (90% probability of death), 0.99, 0.999, 0.9999, and 0.99999 are indicated by solid, dashed, dotted, dot-dashed, and long-dashed lines, respectively. ····· 18

2-7. Comparison of death probability of bacterial population between probability calculation and inactivation kinetic calculation for log-linear (A), downward concavity (B), and upward concavity (C) cases. The lines show the probability calculation and the plot shows the kinetics calculation. The points $P = 0.9$ (90% probability of death), 0.99, 0.999, 0.9999, and 0.99999, indicated by a square, circle, triangle, plus, and cross, are plotted on Fig. 2-6. 19

2-8. Comparison between observed and simulated inactivation of *Salmonella enterica* ser. Agona populations with a mean initial level of $N_0 = 2926$ CFU/ml (A) and $N_0 = 197$ CFU/ml (B). Inactivation was calculated by Monte Carlo simulation (100 simulations) based on Eq. (2-5), Poisson distribution for initial number of cells, and Weibull distribution with parameter b =0.064 and n = 0.981 (A) and b = 0.077 and n =1.002 (B) for individual cell inactivation time. Observed data and no survivors in six trials are indicated by the solid circle and cross, respectively. Experimental data are taken from Aspridou and Koutsoumanis (2015). ····· 20

List of Figures

3-1. Outline of stochastic calculation of the time required for a specific decrease in the number of cells calculated by Eq. (3-5). Upper image shows schematic view of stochastic bacterial inactivation. Lower graph shows changes in probability density of time required to remove a certain number of cells from a population (10 cells). Solid line shows mean time of discrete inactivation of bacterial population. ····· 28

3-2. Stochastic inactivation model of linear model with λ = 0.2×log10 and N_0 = 10 cells. Solid line shows mean value of survivors. Dashed line shows 99% confidence interval of time required for a specific decrease in the number of cells (Eq. (3-6)). ····· 29

3-3. Probability of a population containing survivors when N_0 = 10 cells under inactivation following linear model with λ = 0.2×log10. Solid and dotted lines show probability of a population containing survivors calculated by stochastic approach with individual cell heterogeneity (Eq. (3-7)) and *D*-value approach (Eq. (3-8)). ····· 29

3-4. Outline of stochastic calculation for changing the number of survivors calculated by Eq. (3-10). Upper image shows schematic view of stochastic bacterial inactivation. Lower part shows changes in probability density of number of survivors from a population (20 cells). Solid line shows mean value of viable number of cells in populations. ····· 31

3-5. Stochastic inactivation model with $N_0 = 10^3$ under a linear (A) (b = 0.2×log10, m = 1), downward (B) (b = 0.01×log10, m = 2), and upward curvature (C) (b = 1×log10, m = 0.6). Solid line shows inactivation kinetics. Dashed line shows 0.005 and 0.995 quantiles of Poisson distribution with mean value $N(t) = N_0 e^{-bt^m}$. ····· 33

3-6. Probability of a population containing survivors when N_0 = 10^3 cells under inactivation following a linear (A) (b = 0.2×log10, m = 1), downward (B) (b =0.01×log10, m=2), and upward curvature (C) (b = 1×log10, m = 0.6) model. Solid and dotted lines show probability of a population containing survivors calculated by probabilistic approach with individual cell heterogeneity and initial cell number (Eq. (3-11)) and inactivation kinetics model (Eq. (3-12)). …… 34

3-7. Inactivation kinetic models and probability of a population containing survivors using inactivation kinetics model (b = 0.2×log10, m = 1) with downward concavity (b = 0.01×log10, m = 2) and upward concavity (b = 1×log10, m = 0.6) when N_0 = 10^3 cells. The points $P_{kinetic}(t)$ = 10^{-1} (10% probability of survival), 10^{-2}, 10^{-3}, 10^{-4}, and 10^{-5} are indicated by a square, circle, triangle, plus, and cross, respectively. Dotted lines show example of log-linear approximation. …… 37

3-8. Comparison between observed and theoretically calculated inactivation of *Salmonella enterica* ser. Agona populations with a mean initial level of $N_0 = 2511$ CFU/ml. Solid line shows inactivation kinetics. Bold solid line shows 0.005 and 0.995 quantiles of Poisson distribution with mean value $N(t) = N_0 e^{-bt^m}$. Experimental data and parameters of log-linear model (b = 0.104, m = 1) taken from Aspridou and Koutsoumanis (2015). …… 40

Chapter 1

General Introduction

1.1. Current microbial food safety

Microbiological food safety is continuously improving with our enhanced microbiological knowledge, improved public hygiene, and developments in food processing techniques and food management systems. This progress has led to a marked decrease in the number of foodborne illnesses over recent decades. However, common foodborne pathogens such as *Salmonella, Campylobacter* and *Enterohemorrhagic Escherichia coli* continue to affect millions of people every year (WHO, 2017), and these bacteria affect over 1000 people per year in Japan (Ministry of Health, Labor and Welfare, 2017). Foodborne illnesses occur across the world as a result of new categories of food, complex food chains spanning multiple countries, the evolution of bacterial strains, and environmental changes; each incidence of illness can reveal certain information about foodborne pathogens. Foodborne *Enterohemorrhagic Escherichia coli* and *Salmonella enterica* can cause illness following the ingestion of fewer than 100 cells by people with weak immune systems, such as the elderly and infants (Beuchat et al., 2013; Teunis et al., 2010; Hara-Kudo and Takatori, 2011).

In developing new types of foods, some estimation of their safety is needed. Recently, consumers have requested minimally processed foods with similar or equivalent qualities to the natural and fresh products (Fernández-Sestelo et al., 2013). For example, juices have been sterilized using high pressures instead of thermal inactivation (Vervoort et al., 2011). This reduced processing makes it difficult to control bacterial inactivation or growth (Vervoort et al., 2011). Another example is when new categories of foods come from abroad. In Japan, liquid baby formula and tofu at room temperature have become available in recent years. Some estimation of their safety is needed because every country has different food safety levels. When developing new foods, it is vital to establish their level of safety.

1.2. International food safety framework

In recent decades, an international food safety framework has been promulgated by the Codex Alimentarius Commission and FAO/WHO (Voysey and Brown, 2000; Brown and Stringer, 2002; FAO, 2002). Microbial risk assessment and the Hazard Analysis Critical Control Point (HACCP) system have been introduced to establish food safety standards on a risk-based approach. Microbial risk assessment focuses on reducing the impact of pathogens on healthy individuals. Risk assessment seeks to measure risk and identify its influencing factors. The components of risk assessment are hazard identification, hazard characterization, exposure assessment, and risk characterization. The HACCP system is a food safety management strategy that considers the risk assessment process with the aim of ensuring food safety (Haas et al., 1999). The HACCP system implores producers to consider biological, chemical, and physical hazards in the production process and specifies certain control criteria. This enables problems to be identified before they occur, and establishes measures for their control in terms of food safety (Brown and Stringer, 2002). As the trend toward international exchanges of foodstuffs continues, a comprehensive food safety framework becomes increasingly important. In calculating the degree of risk, probabilistic and stochastic concepts are indispensable modeling tools in the field of food microbiology (Nauta, 2000). Exposure assessments consider the number of survivors as a random variable. Microbial risk assessments consider the bacterial behavior as a probabilistic model, providing more accurate calculations than conventional deterministic approaches.

1.3. Traditional predictive microbiology

Predictive microbiology traditionally considers the deterministic responses of populations of microorganism to environmental factors (e.g., temperature, pH, aw) (Peleg, 2006; Ross and McMeekin, 1994). A primary model describes the changes in cell density over time and a secondary model describes the relationships among kinetic parameters and

environmental factors (McClure et al., 1994; McMeekin et al., 2002). Growth and inactivation models of pathogenic bacteria or spoilage bacteria have been investigated in both the culture medium and the food environment. These deterministic growth and inactivation models are useful for evaluating the processing, distribution, and storage conditions (Ross and McMeekin, 1994). Many growth and inactivation data and models are stored in databases such ComBase (www.combase.cc), making them accessible to industrial, academic, and government researchers.

As primary models, inactivation curves with upward or downward concavity have been developed to simulate observed inactivation behavior (Peleg and Cole, 1998; Xiong et al., 1999). The log-linear model, which is based on thermal inactivation, is still widely used. To summarize the effect of the inactivation rate at different temperatures, some metric such as the decimal reduction time (*D*-value) or *Z*-value is commonly used. The *D*-value is defined by log-linear inactivation, and the *Z*-value is the temperature difference needed to reduce or increase the *D*-value by a factor of 10 (Peleg, 2006). Using these metrics, the commercial sterility of *Clostridium botulinum* has been calculated for retort and canned foods. In addition, the sterilization conditions have been calculated for milk and eggs. Thus, mathematical models are used for a range of practical purposes in food processing.

1.4. Problems with traditional predictive microbiology

Although microbial inactivation does not always follow a log-linear model, the *D*-value is still widely used for risk assessment and estimating the sterilization time (Brown, 2002; Peleg and Normand, 2004). However, the accuracy of *D*-value calculations is uncertain (Koseki et al., 2009; Koyama et al., 2017a; Peleg, 2006). The curvature of the inactivation kinetics means that the *D*-value must be determined manually and subjectively by experts, which leads to some over- or underestimation of bacterial survivors (Peleg, 2006). Thus, the *D*-value might not be appropriate for estimating the probability of a population containing

survivors. In addition, the current model is deterministic, and only provides a point estimation. The random variable of the number of survivors after a given time has not been calculated. In small populations of cells, this random variable is observed because of individual cell heterogeneity. Considering that real foods have low levels of contamination, individual cell heterogeneity should be considered in determining bacterial growth or inactivation behavior. The current deterministic model cannot estimate this random variable. Probabilistic or stochastic models for estimating the random variable should therefore be developed to meet the requirements of microbial risk assessment.

Recently, Aspridou and Koutsoumanis (2015) indicated that the time required for 1-log reduction should not be reported as a single value, but as a probability distribution, once the population has decreased to below 100 cells. The death probability of a bacteria population has also been estimated using a probability distribution (Koyama et al., 2017a). To reflect the real situation, stochastic modeling is often used, because this enables the variability of bacterial behavior to be described (FAO/WHO, 2008; Membré et al., 2006). Taking all the bacterial behavior into consideration, the *D*-value can be changed and we can suggest an appropriate inactivation time. Probabilistic models require variability and uncertainty to estimate bacterial behavior as a probability distribution.

1.5. Variability associated with predictive microbiology

Variability in bacterial behavior is studied because of the risk assessment required for probabilistic models (Brown, 2002; Codex Alimentarius Commission, 2009; FAO/WHO, 2008; Ross and McMeekin, 2003; Voysey and Brown, 2000). There are numerous types of variability observed in the bacterial growth and/or inactivation process. Representative types of variability include the initial contamination level, variability in processing factors, food characteristics such as pH, water activity, environmental factors such as storage temperature, and biological variability such as individual cell heterogeneity and strain variability

(Aspridou and Koutsoumanis, 2015; Delignette-Muller and Rosso, 2000; Schaffner, 2008; van Asselt and Zwietering, 2006; Zwietering, 2002).

One important source of variability comes from individual cells, which can be observed regardless of the growth and/or death of the bacterial population (Baranyi, 2002; Peleg and Cole, 1998). Individual cell heterogeneity manifests as the individual cell inactivation time in inactivation kinetics (Koutsoumanis and Aspridou, 2016). Thus, it is possible to describe individual cell heterogeneity as a probability distribution. Variability in the initial number of cells has been studied experimentally (Aguirre et al., 2009; Koyama et al., 2016; Rodriguez et al., 2016) and computationally (Koyama et al., 2017b). The initial number of cells can be described as a Poisson distribution (Aguirre et al., 2009; Koyama et al., 2017b; Nauta, 2000), which is also used to describe randomly distributed initial cells in ideal conditions (Standaert et al., 2005). These variabilities have all been described as probability distributions, but have not been integrated into inactivation kinetics to overcome the conventional death probability calculation based on the *D*-value.

1.6. Objective of this study

The objective of this study is to calculate and visualize the stochastic nature of individual cells in a population using computer simulations and mathematical modeling. As sources of variability, the individual cell inactivation time and number of initial cells are considered. Chapter 2 describes an approach for simulating individual cell inactivation considering the individual cell heterogeneity and initial number of cells, and estimates the time-to-inactivation and death probability of the bacterial population. In chapter 3, an exponential distribution and Poisson distribution are used to formulate the stochastic inactivation of individual cells in the population and the probability of a population containing survivors in place of the conventional *D*-value.

Chapter 2

Computer Simulation of Inactivation of Bacterial Populations

2. 1. Introduction

The log-linear model and the *D*-value (Peleg, 2006) are used for death probability calculations via a mathematical formula based on the first-order-kinetic assumption. In the case of the probabilistic model, the probability distribution underlying the kinetic model must be considered. Individual cell heterogeneity is described in terms of the kinetic curvature (Koutsoumanis and Aspridou, 2016), and the initial cell number is assumed to follow a statistical distribution (Standaert et al., 2005). Defining variability as a probability distribution from a mathematical viewpoint is a first step toward probabilistic modeling. Bacterial inactivation can then be studied based on this definition to ensure a comprehensive understanding of the process.

The objectives of this study are to illustrate the time-to-inactivation and death probability of bacterial populations via computer simulations while considering the variability in individual cell inactivation times and initial cell numbers. Furthermore, the death probability of the bacterial population is simulated with various initial cell numbers, and the results are compared with those calculated using inactivation kinetics. The proposed approach enables the risk of bacterial survival to be estimated and an appropriate bacterial population death probability selected without using conventional *D*-value extrapolation.

2.2. Materials and Methods

2.2.1. Mathematical-based assumptions

In this study, stochastic population inactivation was simulated under variability in individual cell inactivation times and initial cell numbers. The following two assumptions

were employed in the simulations. First, we assumed that the bacterial inactivation kinetics follow the Weibull inactivation model with an initial N_0 cells (e.g., $N_0 = 10^9$):

$$log_{10}N(t) = -bt^n + log_{10}N_0 \quad (2\text{-}1)$$

where t, $N(t)$, $log_{10}N_0$, b, and n denote the elapsed time, momentary number of survivors at time t, logarithm of number of initial cells, rate, and shape parameter of the Weibull distribution, respectively. The Weibull inactivation model is widely used in investigations of inactivation kinetics (Peleg, 2006; Peleg and Normand, 2004; van Boekel, 2002). Although many survival models have been developed (Xiong et al., 1999), we selected the Weibull model, which can be either concave upward or concave downward to describe bacterial inactivation model. In the case of bacterial inactivation, the individual inactivation time is reflected in the inactivation kinetics (Baranyi and Pin, 2001; Koutsoumanis and Aspridou, 2016; Peleg, 2006). According to the Weibull inactivation model, the inactivation rate of the population changes with time, and the inactivation of individual cells is considered to be an incidental countable event that is independent of other events. Thus, the individual cell inactivation time occurs randomly according to the Weibull probability distribution.

Second, we assumed that the initial number of cells followed a Poisson distribution. If bacterial cells are randomly distributed in a liquid, then the number of bacteria in any portion of that liquid obeys a Poisson distribution (El-Shaarawi et al., 1981; Standaert et al., 2005). When there relatively few cells in a liquid, the cells follow a Poisson distribution (Koyama et al., 2016). Therefore, because of the reproductive property of this distribution type, it is also conceivable that a large amount of cells will follow a Poisson distribution. Third, we assumed that cells could not recover from injury, and so the cells are either alive or dead after a lethal treatment. Under the three assumptions outlined above, we simulated bacterial inactivation with varying individual cell inactivation times and initial cell numbers.

2.2.2. Procedure for computer simulation of bacterial inactivation

In our simulations, we followed the approach of Aspridou and Koutsoumanis (2015), who simulated bacterial inactivation under varying individual cell inactivation times to mimic individual cell heterogeneity. However, we also varied the initial cell number in our computer simulations, thus differentiating the present study from previous simulations. First, we determined the mean value of the initial number of cells N_0 $\{N_0 \in \mathbb{R} \mid N_0 > 0\}$. The initial number of cells in the simulation was generated from a Poisson distribution as follows

$$N_0' \sim Poisson(N_0) \quad (2\text{-}2)$$

where N_0' is the initial number of cells generated from the Poisson distribution with parameter N_0. Next, we estimated the individual cell inactivation time for the N_0' cells. Using inverse transform sampling from the cumulative Weibull distribution with rate and shape parameters, we estimated the individual cell inactivation time t_i of the ith cell as follows:

$$t_i \sim Weibull(b, n), i = 1,2,3 \ldots N_0' \quad (2\text{-}3)$$

For example, when $N_0' = 1000$, random sampling is applied 1000 times to determine the individual cell inactivation time t_i of the ith cell. We then determined the survival or death of the ith cell over time as follows:

$$t < t_i \;\; S_i(t) = 1 \quad \text{(survival)} \quad (2\text{-}4)$$

$$t \geq t_i \;\; S_i(t) = 0 \quad \text{(death)}$$

where $S_i(t)$ denotes the survival or death of the ith cell. Thus, the number of survivors $N(t)$ at time t can be described as follows:

$$N(t) = \sum_1^{N_0'} S_i(t) \quad (2\text{-}5)$$

Equation (2-5) describes one simulated survival curve. To replicate the above simulation, stochastic bacterial inactivation was modeled via Monte Carlo simulations. In this study, we changed the replication method used in the simulation according to the purpose of the

estimation. The R code used for the above stochastic calculation is outlined in the R code viewer (Appendix A).

2.2.3. Trend of time-to-inactivation of bacterial population

To visualize the stochastic inactivation processes and time-to-inactivation, we simulated bacterial inactivation with different Weibull distribution parameters and initial cell numbers. Various parameters such as the inactivation rate, type of inactivation curve, and number of initial cells were examined in the bacterial inactivation simulations (Fig. 2-1, Table 2-1). For each condition, 100 replicates of bacterial inactivation were simulated. In each simulation, the maximum of t_i became a random variable of the time-to-inactivation of the bacterial population. The time-to-inactivation of the bacterial population was used to generate a histogram. Furthermore, we calculated the variance of the time-to-inactivation of the bacterial population for initial cell numbers from 10^0–10^5.

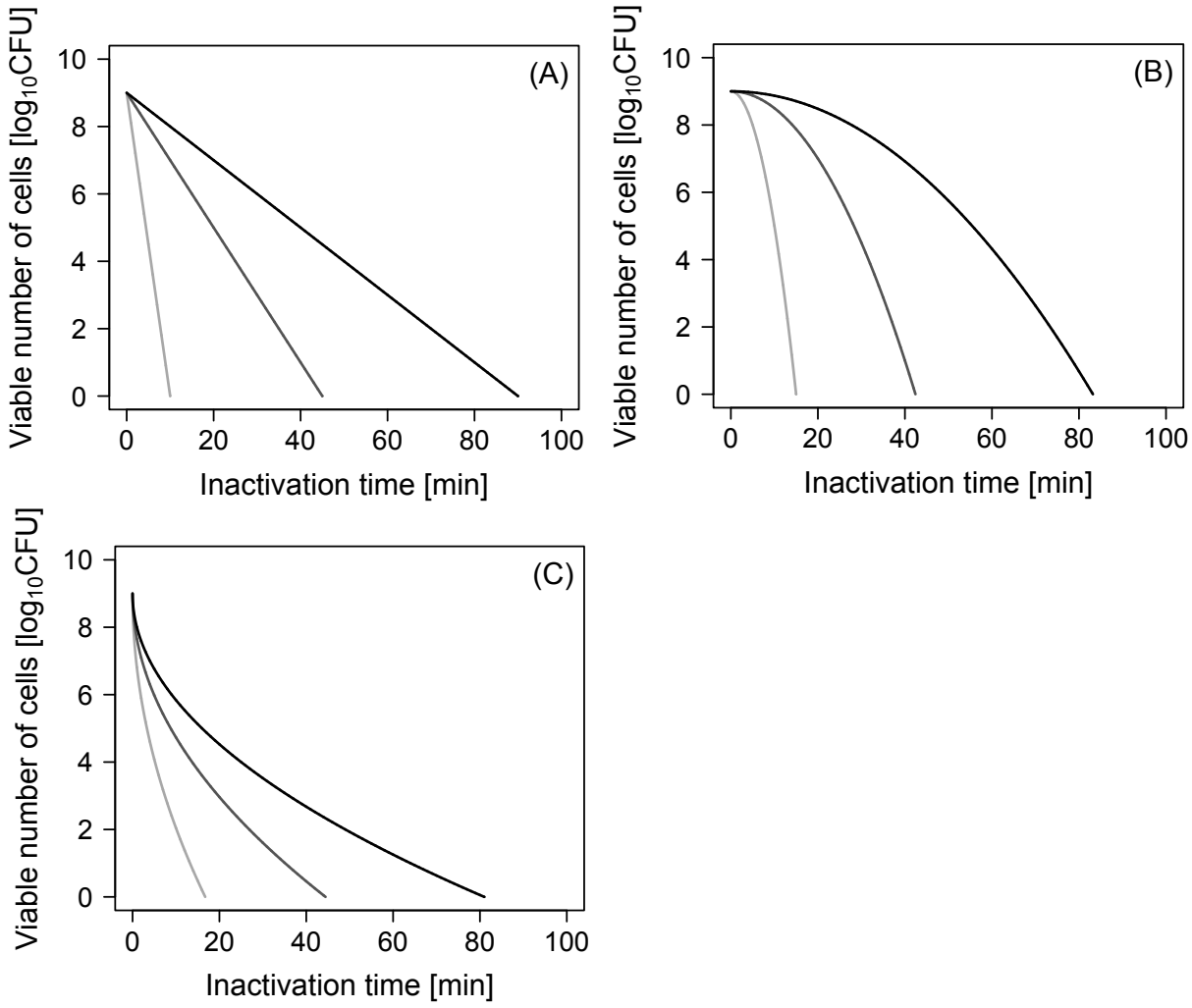


Fig. 2-1. Linear (A), downward concavity (B), and upward concavity (C) log-Weibull models with $N_0 = 10^9$ initial cells.

Table 2-1. Rate parameter b and shape parameters n of Weibull distribution in inactivation kinetics ($log_{10}N(t) = -bt^n + log_{10}N_0$) discussed in this work

Inactivation rate	High		Middle		Low	
Parameter	b	n	b	n	b	n
Linear survival curve	0.9000	1.0	0.2000	1.0	0.1000	1.0
Concave downward curve	0.0400	2.0	0.0050	2.0	0.0013	2.0
Concave upward curve	2.2000	0.5	1.3500	0.5	1.0000	0.5

2.2.4. Death probability of the bacterial population

To estimate the death probability of the bacterial population, we simulated 10^6 replications of bacterial inactivation with initial cell numbers from 10^0–10^5. We then obtained a random variable for the time-to-inactivation from 10^6 replicate simulations. The obtained times-to-inactivation were then sorted from highest to lowest, and the $(10^5+1)th$, $(10^4+1)th$, $(10^3+1)th$, $101th$, and $11th$ values were selected to calculate the certainty level of bacterial inactivation for five levels of death probability of the bacterial population, ranging from 90–99.999%. To visualize the death probability of the various numbers of initial cells, contour lines were plotted. In addition, the death probability of the bacterial population was calculated directly from the inactivation kinetics curve. The death probability calculation using the inactivation kinetics curve is analogous to the extrapolation of the *D*-value. Methods that extrapolate the *D*-value use the survival numbers of the bacterial population as the survival probability when the number of survivors is less than one. Thus, the death probability of a bacterial population P is described as $\{P = 1 - N(t) \mid N(t) \leq 1\}$. The inactivation time computed from Eq. (2-1) is as follows:

$$t_{Inact}(P) = \sqrt[n]{\frac{1}{b} log_{10}(\frac{1}{1-P})}, P = 0.9,0.99,0.999,0.9999,0.99999 \qquad (2\text{-}6)$$

where $t_{Inact}(P)$ is the inactivation time for the death probability of bacterial population P. The representative death probability of the bacterial population estimated from the kinetics model is illustrated in Fig. 2-2. Thus, the death probabilities given by the kinetic and stochastic models can easily be compared.

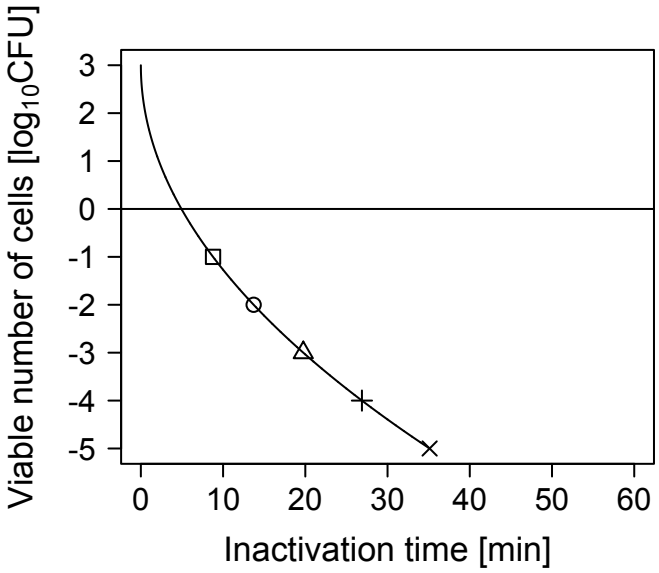


Fig. 2-2. Death probability estimation using inactivation kinetics model ($N_0 = 10^3, b = 1.35, n = 0.5$). The points P = 0.9 (90% probability of death), 0.99, 0.999, 0.9999, and 0.99999 are indicated by a square, circle, triangle, plus, and cross, respectively.

2.2.5. Validation of bacterial inactivation behavior

To validate our simulation results, we compared them with experimental data from a previous study (Aspridou and Koutsoumanis, 2015). The acid inactivation of *Salmonella enterica* ser. Agona with initial cell concentrations of approximately 3.4 $\log_{10}$CFU/ml and 2.3 $\log_{10}$CFU/ml was measured in acidified tryptone soy broth with lactic acid (pH 3.5). The inactivation experiments included nine independent trials at each initial cell level. We used data from three trials for the computer simulations with the Weibull model, and used the results from the other six trials for validation. We fixed the initial cell level N_0 as the mean value of the three trials and fitted the experimental data using the Weibull model (Eq. (2-1)) to minimize the root mean square error (RMSE). We simulated the inactivation of *Salmonella enterica* ser. Agona populations using the mean initial level of the validation data, 2926 CFU/ml and 197 CFU/ml, with a Poisson distribution for the initial cell number and the fitted

Weibull model for the individual cell inactivation times. We then compared our computational results with the experimental data. All statistical analyses were conducted using the R statistical software (Version 3.4.2 for Mac OS X; http://ww.r-project.org).

2.3. Results

In all the tested conditions, the stochastic inactivation process and the time-to-inactivation of the bacterial population were successfully determined (Figs. 2-3 and 2-4). The trend in the time-to-inactivation of the bacterial population varied depending on the initial number of cells and the shape and rate parameters of the Weibull distribution. As the inactivation rate decreased, the variance of the time-to-inactivation increased, regardless of the type of curve (Fig. 2-5). In contrast, the variance of the time-to-inactivation depended on the type of inactivation curve and the initial number of cells. As the number of initial cells increased, the variance of the time-to-inactivation remained almost constant in the case of the log-linear model. In the case of downward and upward concavity, the variance of the time-to-inactivation decreased and increased as the number of initial cells increased (Fig. 2-5).

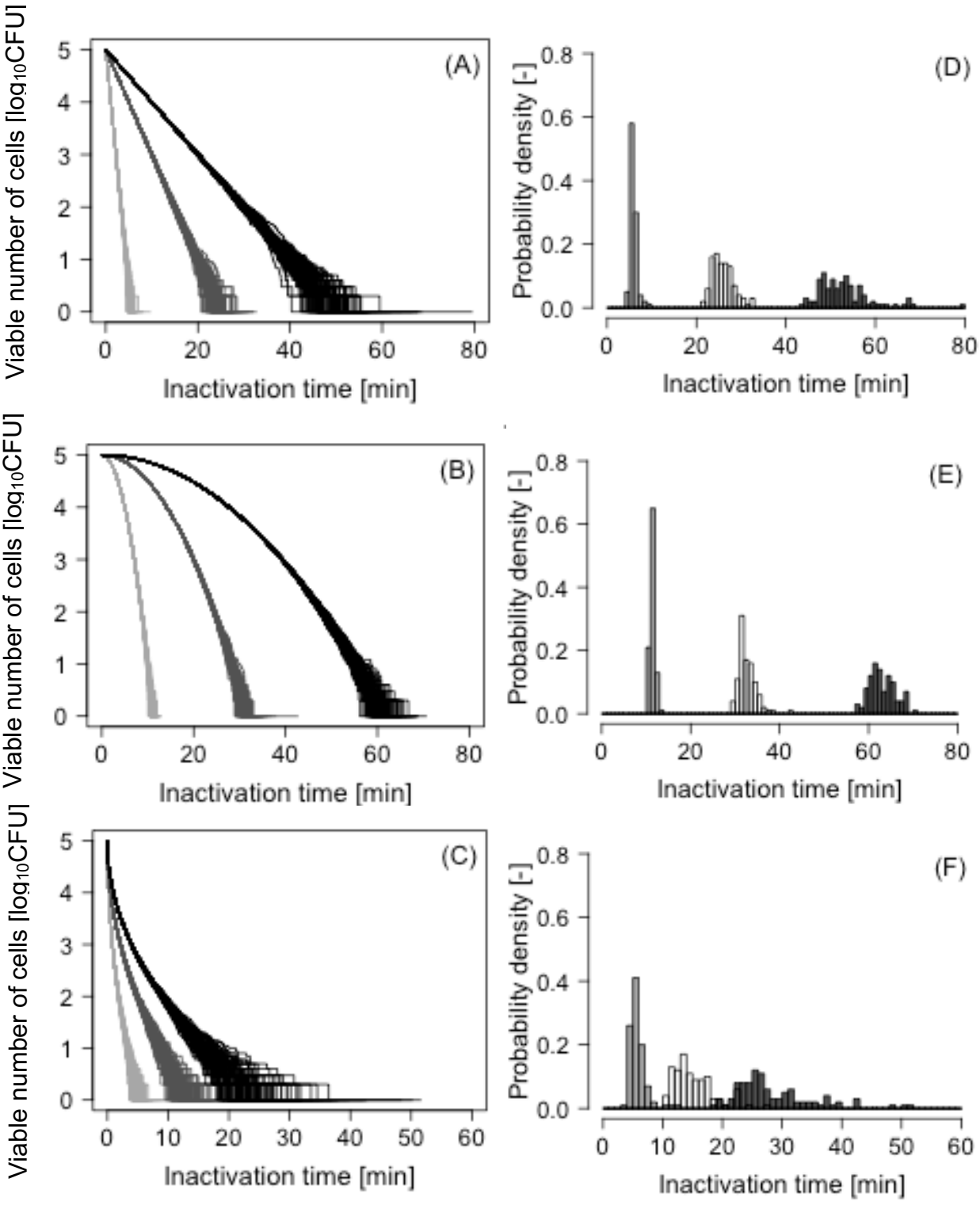


Fig. 2-3. (Top row) Monte Carlo simulation results (100 simulations) for the linear (A), downward concavity (B), and upward concavity (C) inactivation curves with $N_0 = 10^5$ initial cells. (Bottom row) Histograms showing time-to-inactivation of bacterial population for the linear (D), downward concavity (E), and upward concavity (F) inactivation curves.

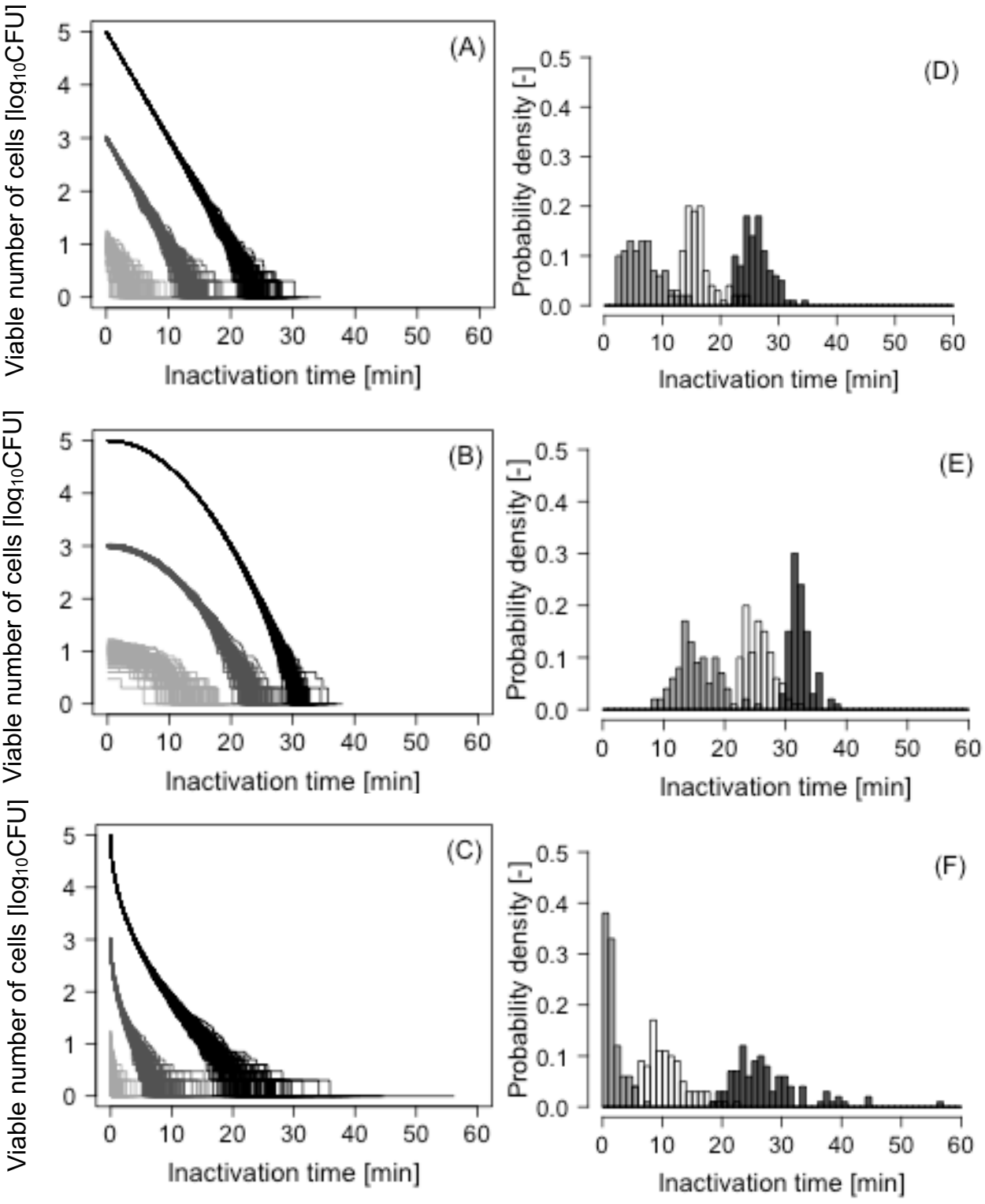


Fig. 2-4. (Top row) Monte Carlo simulation results (100 simulations) for the linear ($b = 0.2, n = 1$) (A), downward concavity ($b = 0.005, n = 2$) (B), and upward concavity ($b = 1, n = 0.5$) (C) inactivation curves with $N_0 = 10, 10^3, 10^5$ initial cells. (Bottom row) Histograms showing time-to-inactivation of bacterial population for the linear (D), downward concavity (E), and upward concavity (F) inactivation curves.

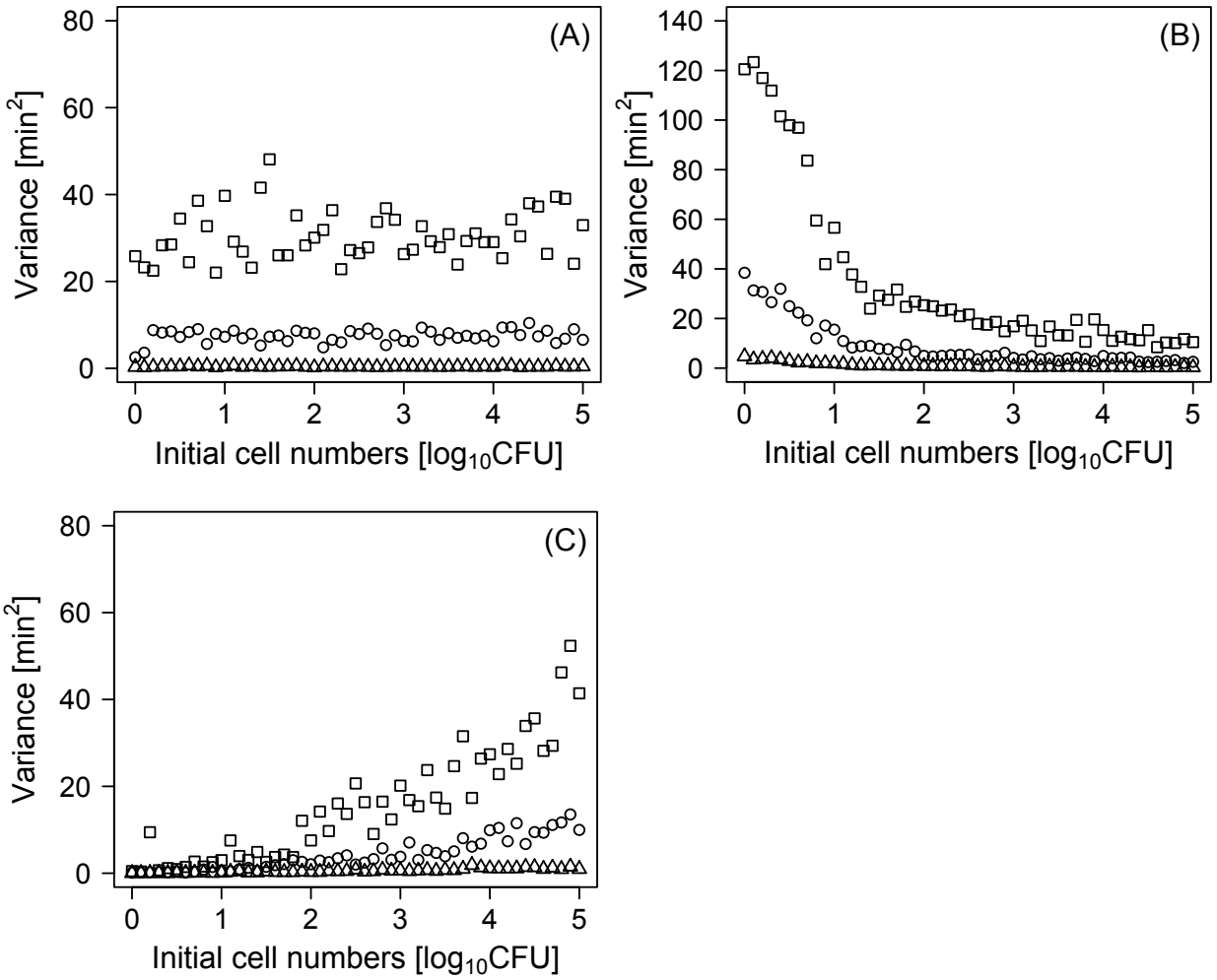


Fig. 2-5. Variance of time-to-inactivation of bacterial population (100 simulations) with various numbers of initial cells for log-linear (A), downward concavity (B), and upward concavity (C) cases. The low, middle, and high inactivation rates of the kinetics are indicated by a square, circle, and triangle, respectively.

To summarize the death probability with respect to the initial number of cells, we described the death probability of the bacterial population as an interface (Fig. 2-6). The target number of cells was described as a negative value of the initial number of cells (Figs. 2-6 and 2-7). The death probability contour line for the log-linear model exhibited a linear relationship between time and the targeted initial cell reduction (Fig. 2-6). In contrast, the death probability contour line for the downward or upward concavity cases did not exhibit a linear relationship between time and the targeted initial cell reduction (Fig. 2-6). The trend in the contour line of the death probability had the same curvature as the inactivation kinetics (Figs. 2-1 and 2-6). We compared the death probability of the bacterial population calculated via inactivation kinetics with that given by the stochastic model developed in this study. The contour line of the death probability was almost congruent with the inactivation kinetics calculation (Fig. 2-7). This indicates that the death probability of the bacterial population can be estimated from the kinetic model, as in Fig. 2-2. The best fit parameters for the 3.4 $\log_{10}$CFU/ml level are b = 0.064 and n = 0.970, which give an RMSE of 0.172, and those for the 2.3 $\log_{10}$CFU/ml level are b = 0.087 and n = 0.914, which give an RMSE of 0.151. The validation results are shown in Fig. 2-8. The observed data (●) are broadly consistent with the simulation results in the regions where a number of survivors are expected. Instances of no survivors after six trials (×) mostly occur after the simulations have finished, when no survivors are expected. Thus, our simulation model can describe the variability in the inactivation behavior of the population.

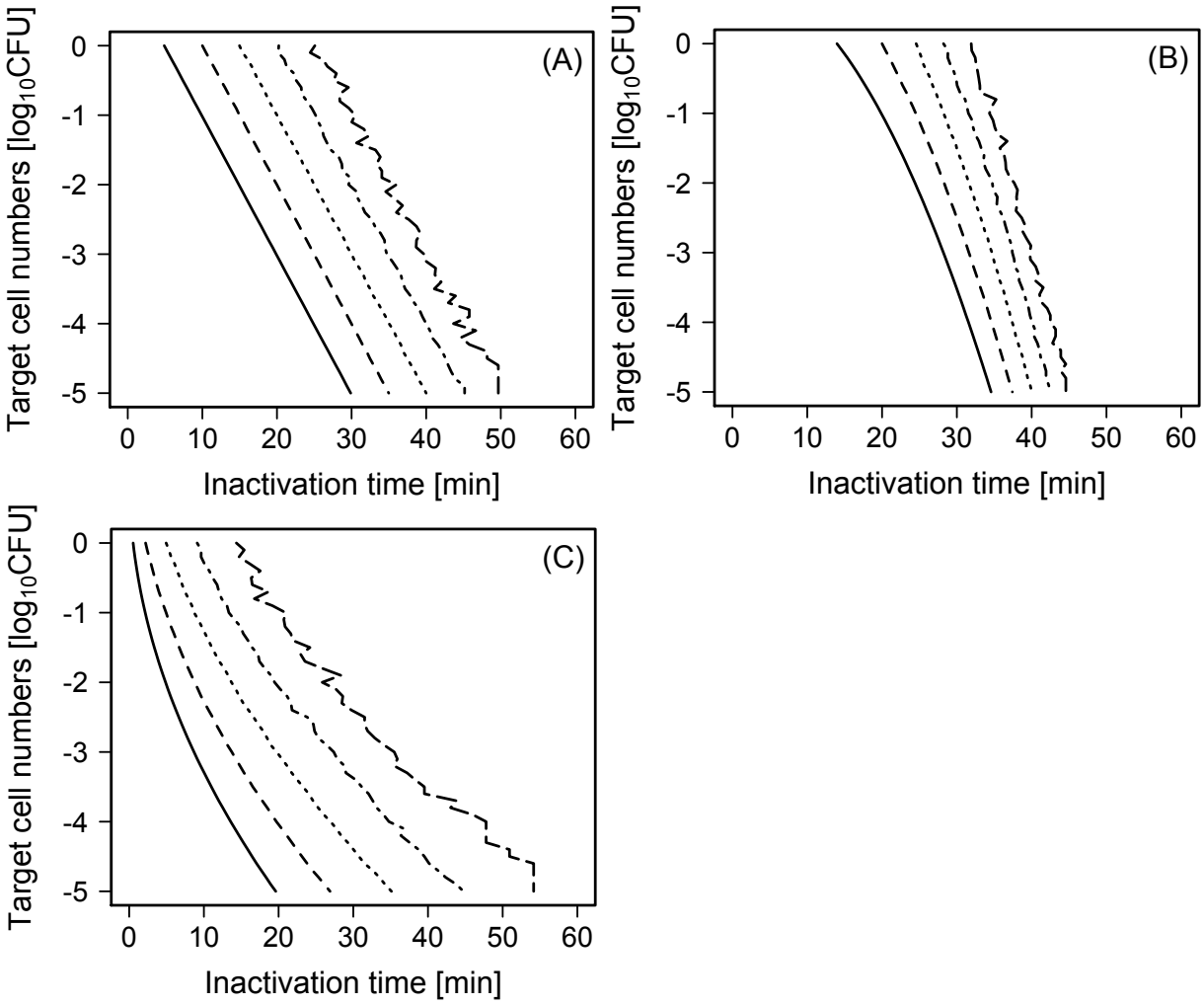


Fig. 2-6. Representation of the death probability of bacterial population for log-linear ($b = 0.2, n = 1$) (A), downward concavity ($b = 0.005, n = 2$) (B), and upward concavity ($b = 1.35, n = 0.5$) (C) cases calculated via our stochastic approach. The interfaces $P = 0.9$ (90% probability of death), 0.99, 0.999, 0.9999, and 0.99999 are indicated by solid, dashed, dotted, dot-dashed, and long-dashed lines, respectively.

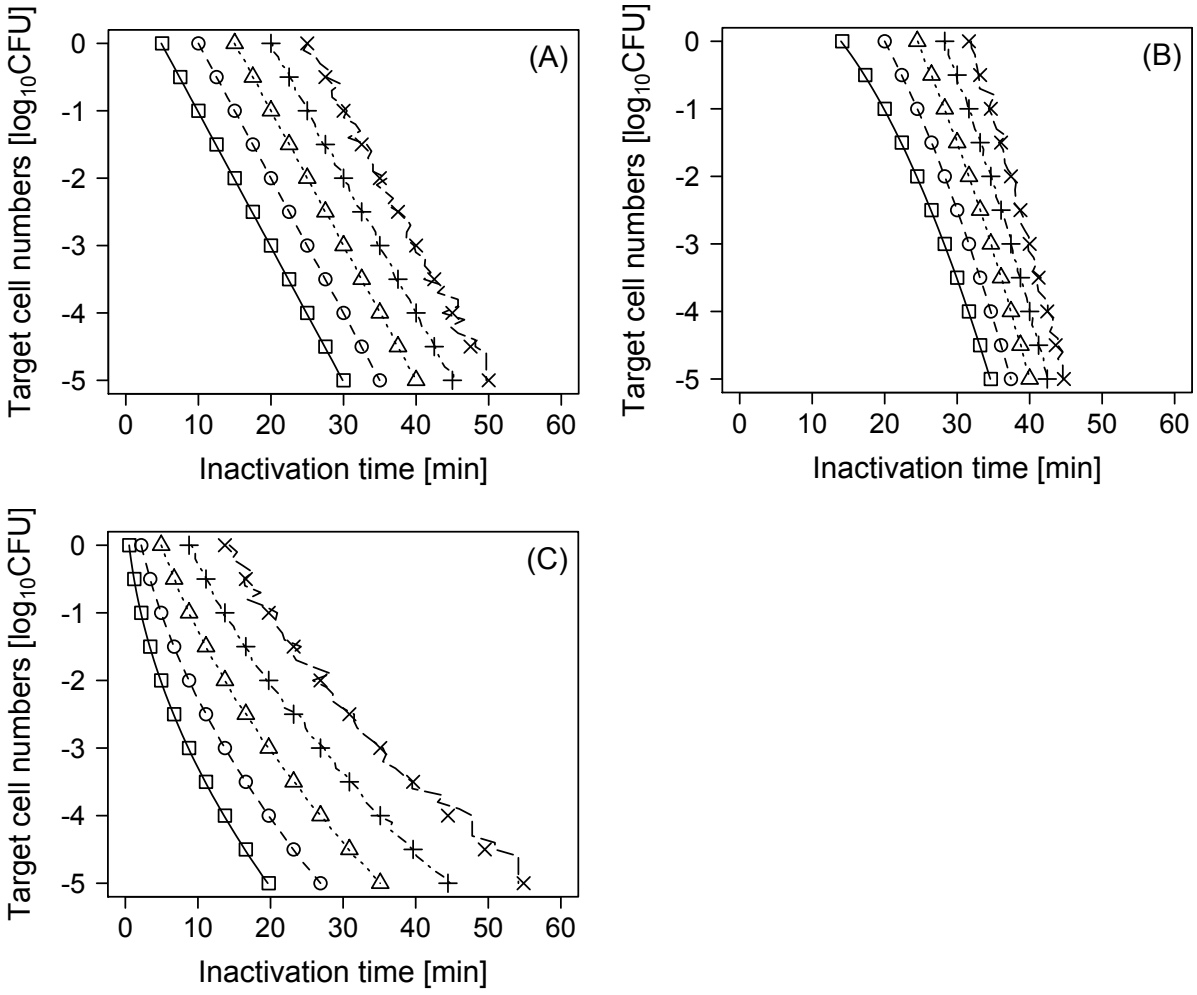


Fig. 2-7. Comparison of death probability of bacterial population between probability calculation and inactivation kinetics calculation for log-linear (A), downward concavity (B), and upward concavity (C) cases. The lines show the probability calculation and the plot shows the kinetics calculation. The points $P = 0.9$ (90% probability of death), 0.99, 0.999, 0.9999, and 0.99999, indicated by a square, circle, triangle, plus, and cross, are plotted on Fig. 2-6.

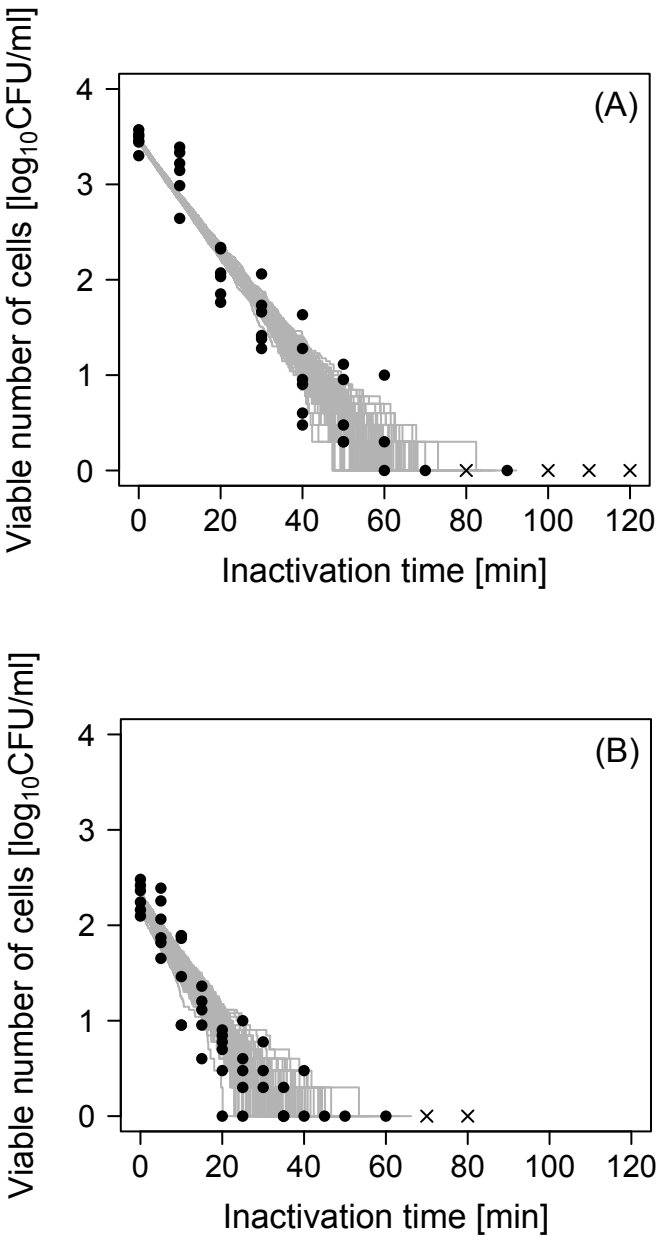


Fig. 2-8. Comparison between observed and simulated inactivation of *Salmonella enterica* ser. Agona populations with a mean initial level of $N_0 = 2926$ CFU/ml (A) and $N_0 = 197$ CFU/ml (B). Inactivation was calculated with Monte Carlo simulation (100 simulations) based on Eq. (2-5), Poisson distribution for initial number of cells, and Weibull distribution with parameters b =0.064 and n = 0.981 (A) and b = 0.077 and n =1.002 (B) for individual cell inactivation time. Observed data and no survivors in six trials are indicated by the solid circles and crosses, respectively. Experimental data are taken from Aspridou and Koutsoumanis (2015).

2. 4. Discussion

In this study, we simulated bacterial inactivation for various individual cell inactivation times and initial numbers of cells. In all the tested conditions, the time-to-inactivation of the bacterial population was successfully simulated (Figs. 2-3 and 2-4). The variance of the time-to-inactivation was found to depend on the type of inactivation curve (Fig. 2-5). In addition, we successfully derived the death probability of the bacterial population (Fig. 2-6), and found that this is virtually the same as that obtained via the kinetics calculation (Fig. 2-7). The stochastic model proposed in this study indicates that the conventional inactivation kinetics model enables the death probability of the bacterial population to be accurately estimated (Fig. 2-2). Furthermore, we validated our computer simulations using experimental data from the literature (Fig. 2-8). Thus, we have estimated the death probability of the bacterial population based on inactivation kinetics curves instead of the extrapolation of the *D*-value.

The time-to-inactivation has not been estimated as a probability distribution by the conventional kinetics model. In this study, the variability in the time-to-inactivation was described using histograms. Further, the trend in time-to-inactivation was visualized using various Weibull distribution parameters and initial numbers of cells (Figs. 2-3 and 2-4). The shape of the inactivation curve and the inactivation speed were shown to significantly influence the time-to-inactivation (Figs. 2-3 and 2-4). For example, a low inactivation rate causes the bacteria to live longer than a high inactivation rate, regardless of the type of curvature (Fig. 2-3). With a high initial number of cells, the bacteria survive longer and have a higher variance in the case of an upward concave curve (Fig. 2-4). These trends cannot be estimated from calculations based on extrapolating the *D*-value. The above information is useful for determining the risk of bacterial survivors after the inactivation process.

The initial number of cells was described as a Poisson distribution in this study (Eq. (2-2)). In conducting risk assessments, the initial number of cells should be described using a probability distribution (Nauta, 2002). The Poisson distribution was used to express

variability in the initial number of cells (Nauta, 2000), and we simulated stochastic inactivation of the bacterial population where the initial number of cells follows a Poisson distribution. The number of surviving cells was also described by a Poisson distribution under the assumption that the initial cells, which obey a Poisson distribution, randomly die (Aguirre et al., 2009). In our model, the individual cell inactivation times are independent (Eq. (2-3)). Thus, the number of survivors simulated in this study follows a Poisson distribution, regardless of the parameters of the Weibull distribution and the initial number of cells. In addition, the Poisson distribution allows us to set the initial cell number as a real number, rather than being limited to integer values. The approach proposed in this study not only estimates the death probability of bacterial populations, but also calculates the number of survivors. This is important, because both values are required for exposure assessments (Brown, 2002). A more flexible mechanism for setting the number of initial cells, permitting distributions other than the Poisson distribution, would allow the computer simulations for risk assessment to be significantly expanded.

The procedure for calculating the *D*-value ignores the inactivation curve (Peleg, 2006). This is one of the reasons why the *D*-value cannot precisely estimate the death probability of a bacterial population. Considering the inactivation curvature, we calculated the death probability of the bacterial population using a probabilistic approach based on the inactivation curve (Figs. 2-2 and 2-6). The results indicate that the death probability of the bacterial population enables estimations to be formed from the inactivation curve (Fig. 2-7). Thus, conventional death kinetics studies have reported that time can be incorporated into the death probability calculation. While the previous probabilistic model requires new and additional experimental data (Koyama et al., 2017a) and has a complex calculation process, the calculation procedure presented in this study is relatively simple (Eq. (2-6)). Thus, its application to probabilistic evaluations for databases such as ComBase is easier because the only additional requirement is the kinetic model.

In this study, the time-to-inactivation and death probability of the bacterial population were described via computer simulations based on a mathematical approach. The proposed approach enables us to discuss the death probability of the bacterial population based on probability theory, unlike traditional calculations that extrapolate deterministic approaches. To transform the deterministic approach into a probabilistic or stochastic model, a mathematical approach is important. In addition, computer simulations are important for visualizing the complex scenarios described by stochastic formulations. The stochastic growth model and growth/no-growth model can also be discussed in terms of a combination of mathematical approaches and computer simulations from the aspect of probability theory. For example, variability in the growth behavior can be calculated and simulated using exponential growth kinetics. Our stochastic simulation for the death probability of bacterial populations can help to estimate the risk of bacterial survivors without any need for the *D*-value concept.

Chapter 3

Mathematical Modeling of Inactivation

3.1. Introduction

Conventional probabilistic approaches employ statistical analysis based on observed data, but they cannot be applied to various inactivation cases for which there is no probabilistic theory behind the bacterial behavior. For example, variability in the number of survivors or the time required for a specific decrease in the number of cells has not been described mathematically. These previous studies do not consider variability in the population dynamics, although they have constructed a stochastic inactivation model based on mathematical aspects including the activation/inactivation of spores and the injury/recovery of cells (Corradini et al., 2010a; 2010b; Horowitz et al., 2009; Peleg, 2016). A systematic mathematical approach is vital in providing an understanding of the variability in observed bacterial inactivation, regardless of bacterial strains or environmental conditions.

In the present study, we focused on variability in the individual cell inactivation times and initial cell numbers. We considered the Weibull inactivation model as one of the simplest examples, providing curves with upward and downward concavity in the inactivation model. Based on the variability of the inactivation times and number of cells, we calculated the stochastic inactivation process. The assumptions regarding the variability were defined as follows:

(A) The individual cell inactivation time follows a Weibull or exponential distribution.

(B) The initial number of cells follows a Poisson distribution.

(C) Cells do not recover from injury and are either alive or dead after the lethal treatment.

Cumulative inactivation can be considered as the aggregation of individual cell inactivation (Peleg, 2006), which can be defined as individual cell heterogeneity in the kinetics model (Koutsoumanis and Aspridou, 2017). According to the nature of the exponential and Weibull distributions, bacterial inactivation was considered to be an incidental countable event that is independent of other events. In addition, the initial cell number was considered. The number of bacteria in inoculum obeys a Poisson distribution (Aguirre et al., 2009; Francois et al., 2005; Koyama et al., 2017b; Nauta, 2000) when a certain volume of liquid can be taken from the inoculum. Thus, we examined the variability in individual cell inactivation times and initial cell numbers to calculate the stochastic inactivation of a bacterial population.

The objective of this study was to calculate the probability of a population containing survivors via a stochastic inactivation process, rather than using the conventional *D*-value estimation. The variability in individual cell inactivation times and the initial number of cells were taken into consideration for the stochastic calculation. The time required for a specific decrease in the number of cells and the number of survivors was calculated as a probability distribution via a stochastic formulation. The proposed stochastic formulation would enable an appropriate probability of a population containing survivors to be determined as an alternative to the conventional *D*-value.

3.2. Material and Methods

3.2.1. Stochastic calculation of the time required for a specific decrease in the number of cells

In this section, the stochastic inactivation process is calculated for a linear model using the variability in the individual cell inactivation times. Let N_0 be the initial number of bacterial cells and $N(t)$ be the number of survivors at time t. The inactivation of a cell population is described as follows:

$$N(t) = N_0 e^{-\lambda t} \tag{3-1}$$

where λ is a rate parameter of the exponential distribution. The probability density of the exponential distribution $f(t)$, which indicates the individual cell inactivation time, is described as:

$$f(t) = \lambda e^{-\lambda t} \tag{3-2}$$

We reproduce the stochastic inactivation process based on the theory that the individual cell inactivation times are independent of other events. First, we calculate the timing of a single-cell decrease in a population of n cells ($n \in \mathbb{N}$). The n cells become $n-1$ cells after one cell inactivation. The momentary failure rate of a cell in the population is equal to the sum of the failure rate of all cells, because the momentary failure rate λ is independent of the other cells' inactivation. Thus, the failure rate of a population with n individuals can be described as $n\lambda$. From Eq. (3-2), the timing of a single-cell decrease in a population of n cells can be described as:

$$f_{n,n-1}(t) = n\lambda e^{-n\lambda t} \tag{3-3}$$

where $f_{n,n-1}(t)$ is the probability density distribution of the timing of a single-cell decrease in a population of n cells. Next, we consider the serial inactivation of multiple cells. According to Eq. (3-3), the timing of a single-cell decrease can be described using the exponential distribution. As each inactivation process is independent of any other inactivation, the random variable of each inactivation process can be summed to calculate the time required for the population to decrease by any given number of cells. Thus, the time required for a specific decrease in the number of cells is calculated as the sum of random variables of the exponential distributions. The sum of random variables of independent distributions is the convolution of distributions. The convolution of exponential distributions can be calculated as follows. Let $X_1, \dots, X_k$ be independent random variables representing the exponential distribution with parameter β_i $(i = 1, 2, \dots, k)$. In general, the sum of multiple

variables of exponential distributions ($S_k = X_1 + \cdots + X_k$) is given by the convolution of the exponential distributions (Akkouchi, 2008; Kulkarni, 2016):

$$f_{S_k}(t) = \sum_{i=1}^{k} \frac{\beta_1 \ldots \beta_k}{\prod_{\substack{j=1 \\ j \neq i}}^{k} (\beta_j - \beta_i)} \exp(-t\beta_i) \quad (3\text{-}4)$$

where $n\lambda \ldots N_0\lambda$ have been substituted for $\beta_1 \ldots \beta_k$. The time required for N_0 initial cells to become $n-1$ surviving cells is as follows:

$$f_{N_0,n-1}(t) = n\binom{N_0}{n}\lambda \sum_{i=n}^{N_0} (-1)^{i-n}\binom{N_0-n}{i-n} e^{-\lambda i t} \quad (3\text{-}5)$$

Using Eq. (3-5), the time-to-inactivation of N_0 cells is then described as:

$$f_{N_0,0}(t) = N_0\lambda \sum_{i=1}^{N_0} (-1)^{i}\binom{N_0-1}{i-1} e^{-\lambda i t} \quad (3\text{-}6)$$

A schematic view of the above calculation is given in Fig. 3-1.

Using Eq. (3-6), the probability of a population containing survivors from an initial number of N_0 cells is given by:

$$P_{stochastic1}(t) = 1 - \int_0^t f_{N_0,0}(t)\, dt \quad (3\text{-}7)$$

where $P_{stochastic1}(t)$ is the probability of a population containing survivors calculated via the time required for a specific decrease in the number of cells. From Eq. (3-5), we can describe the stochastic bacterial inactivation as a discrete process (Fig. 3-2). From Eq. (3-7), we can describe the probability of a population containing survivors (Fig. 3-3). The probability of a population containing survivors can also be calculated directly from the *D*-value (Fig. 3-3). The probability of a population containing survivors is described using the *D*-value as:

$$P_{D-value}(t) = N_0 10^{-\frac{t}{D}} \ (N(t) < 1) \quad (3\text{-}8)$$

$$P_{D-value}(t) = 1 \ \ (N(t) \geq 1)$$

where D and $P_{D-value}(t)$ are the *D*-value and the corresponding probability of a population containing survivors, respectively.

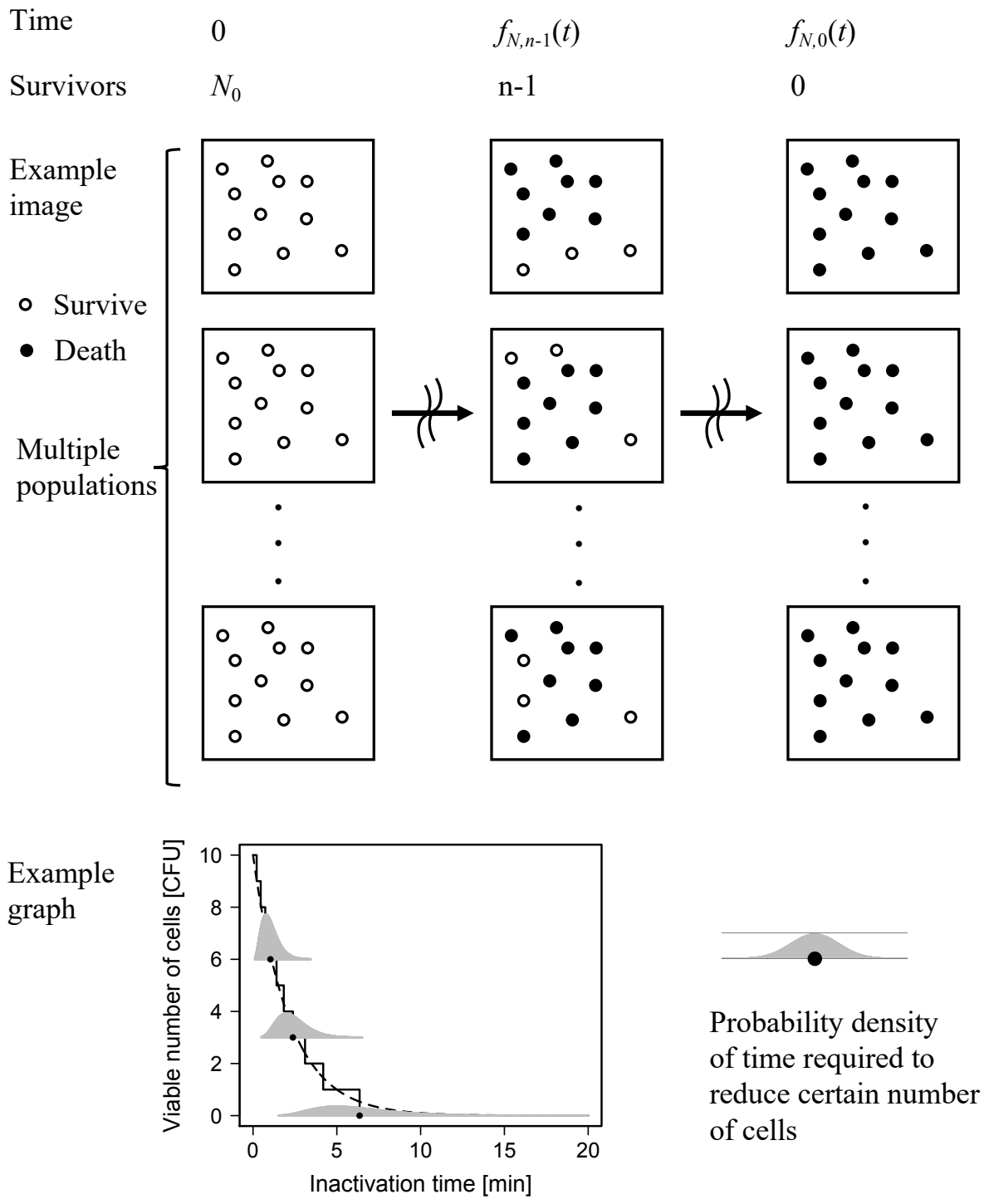


Fig. 3-1. Outline of stochastic calculation of the time required for a specific decrease in the number of cells calculated by Eq. (3-5). Upper image shows schematic view of stochastic bacterial inactivation. Lower graph shows changes in probability density of time required to reduce certain number of cells from a population (10 cells). Solid line shows mean time of discrete inactivation of bacterial population.

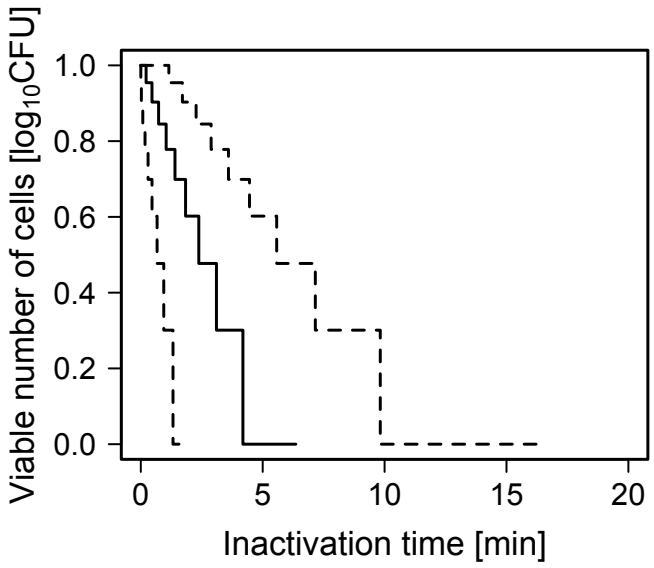


Fig. 3-2. Stochastic inactivation model of linear model with λ = 0.2×log10 and N_0 = 10 cells. Solid line shows mean value of survivors. Dashed line shows 99% confidence interval of time required for a specific decrease in the number of cells (Eq. (3-6)).

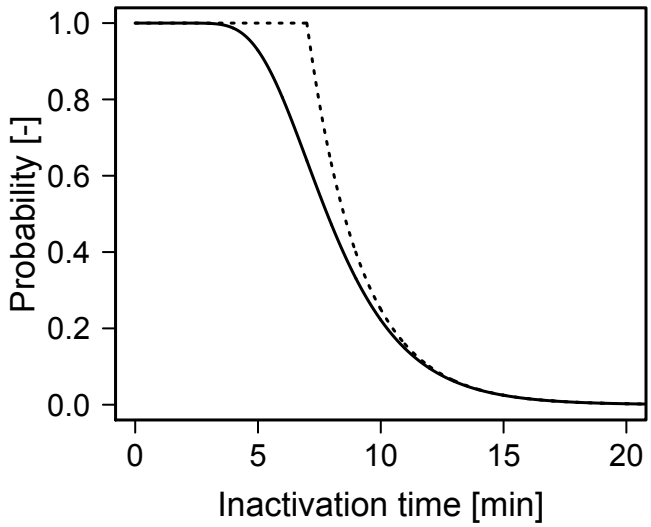


Fig. 3-3. Probability of a population containing survivors when N_0 = 10 cells under inactivation following linear model with λ = 0.2×log10. Solid and dotted lines show probability of a population containing survivors calculated by stochastic approach with individual cell heterogeneity (Eq. (3-7)) and *D*-value approach (Eq. (3-8)).

3.2.2. Stochastic calculation for changing the number of survivors

The stochastic inactivation process can be calculated by combining variability in the individual cell inactivation time with that in the initial cell number. Stochastic changes in the number of survivors are calculated for the Weibull model. Each event is independent of other events in the Weibull distribution, which means that bacteria die randomly throughout the inactivation process. Our process shows that the initial cell number follows a Poisson distribution and that the survivors die uniformly at random. Under the assumption that the initial cells (which follow the Poisson distribution) die at random, the number of surviving cells also follows a Poisson distribution (Aguirre et al., 2009). Based on this theory, the survivors follow a Poisson distribution. The Weibull model can be written as:

$$N(t) = N_0 e^{-bt^m} \tag{3-9}$$

where b and m denote the rate and shape parameters of the Weibull distribution, respectively. We describe the survivors using a Poisson distribution, where the mean value is given by the kinetics model (Eq. (3-9)) as follows:

$$N'(t) \sim Poisson(N(t)) \tag{3-10}$$

$$P(X = k) = \frac{N(t)^k \exp(-N(t))}{k!}$$

where $N'(t)$ and $P(X = k)$ are the number of survivor at time t and the probability of the number of survivors k. A schematic view of the above calculation is shown in Fig. 3-4.

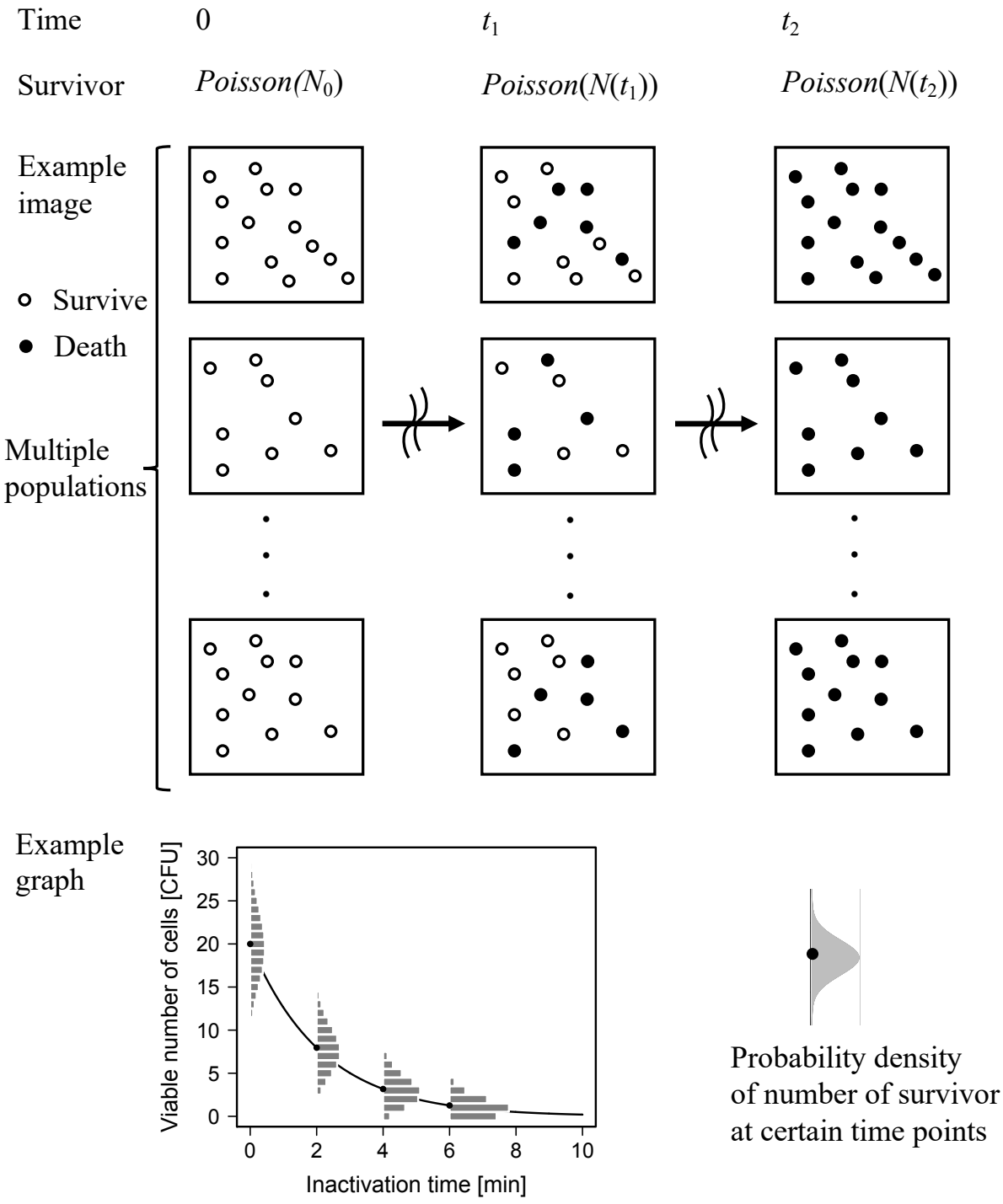


Fig. 3-4. Outline of stochastic calculation for changing the number of survivors calculated by Eq. (3-10). Upper image shows schematic view of stochastic bacterial inactivation. Lower part shows changes in probability density of number of survivors from a population (20 cells). Solid line shows mean value of viable number of cells in populations.

We set $k = 0$ in Eq. (3-10) to calculate the death probability of the bacterial population. The probability of a population containing survivors is then calculated as follows:

$$P_{stochastic2}(t) = 1 - \exp(-N(t)) \quad (3\text{-}11)$$

where $P_{stochastic2}(t)$ is the probability of a population containing survivors calculated by the stochastic change in the number of survivors. From Eq. (3-10), we can describe the bacterial inactivation process (Fig. 3-5). The probability of a population containing survivors is described by Eq. (3-11) (Fig. 3-6). In addition, the probability of a population containing survivors can be calculated using inactivation kinetics (Eq. (3-9)) as follows:

$$P_{kinetic}(t) = N_0 e^{-bt^m} \ (N(t) < 1) \quad (3\text{-}12)$$

$$P_{kinetic}(t) = 1 \ (N(t) \geq 1)$$

where $P_{kinetic}(t)$ is the probability of a population containing survivors calculated via the inactivation kinetics model. Further, we calculated the difference in the probability of a population containing survivors when calculated using the inactivation kinetics and the stochastic model with $\{(P_{kinetic}(t) - P_{stochastic2}(t)) / P_{kinetic}(t)\}$ (Table. 3-1). All statistical analyses were conducted using the R statistical software (Version 3.4.2 for Mac OS X; http://www.r-project.org).

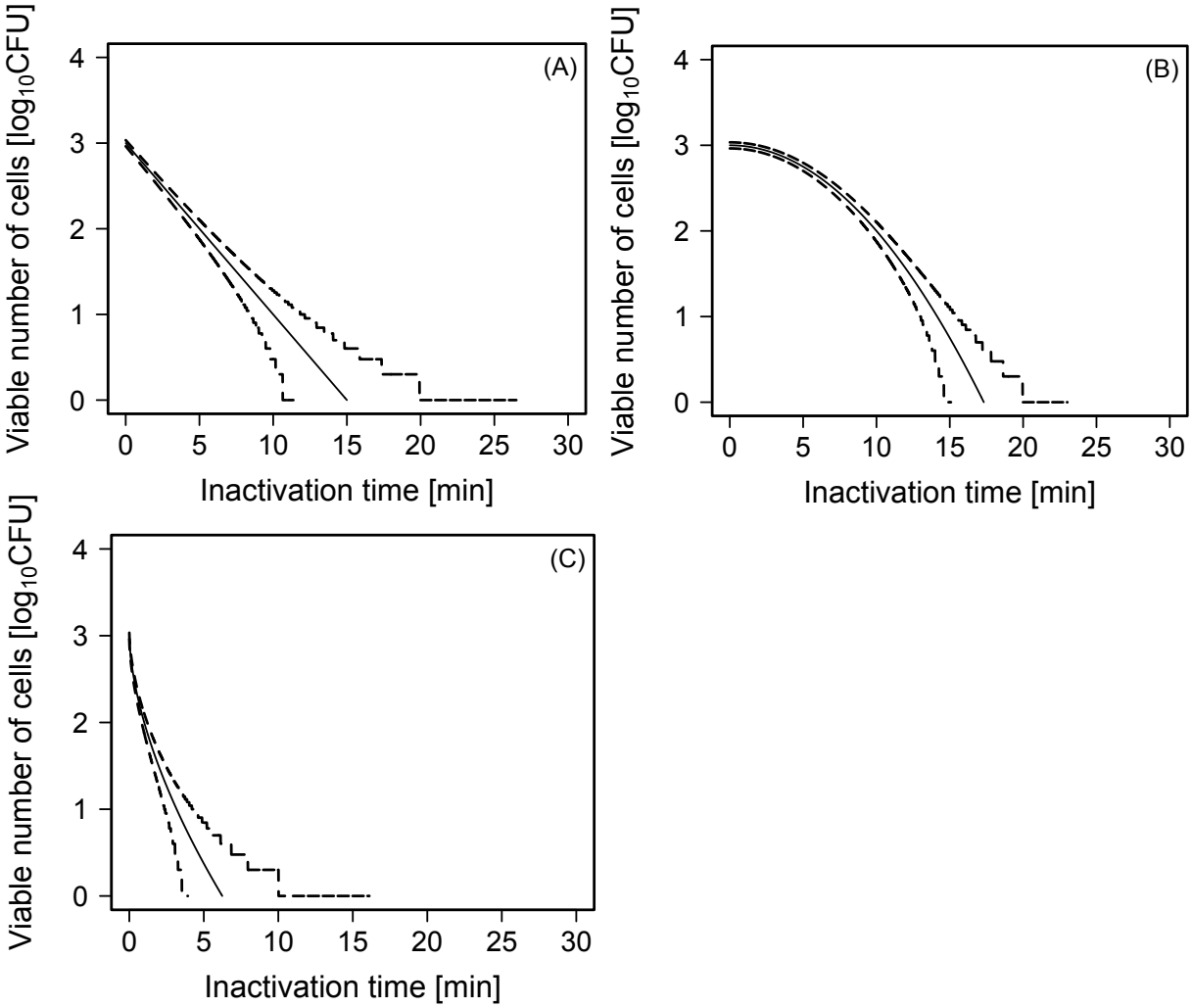


Fig. 3-5. Stochastic inactivation model with $N_0 = 10^3$ under a linear (A) (b = 0.2×log10, m = 1), downward (B) (b = 0.01×log10, m = 2), and upward curvature (C) (b = 1×log10, m = 0.6). Solid line shows inactivation kinetics. Dashed line shows 0.005 and 0.995 quantiles of Poisson distribution with mean value $N(t) = N_0 e^{-bt^m}$.

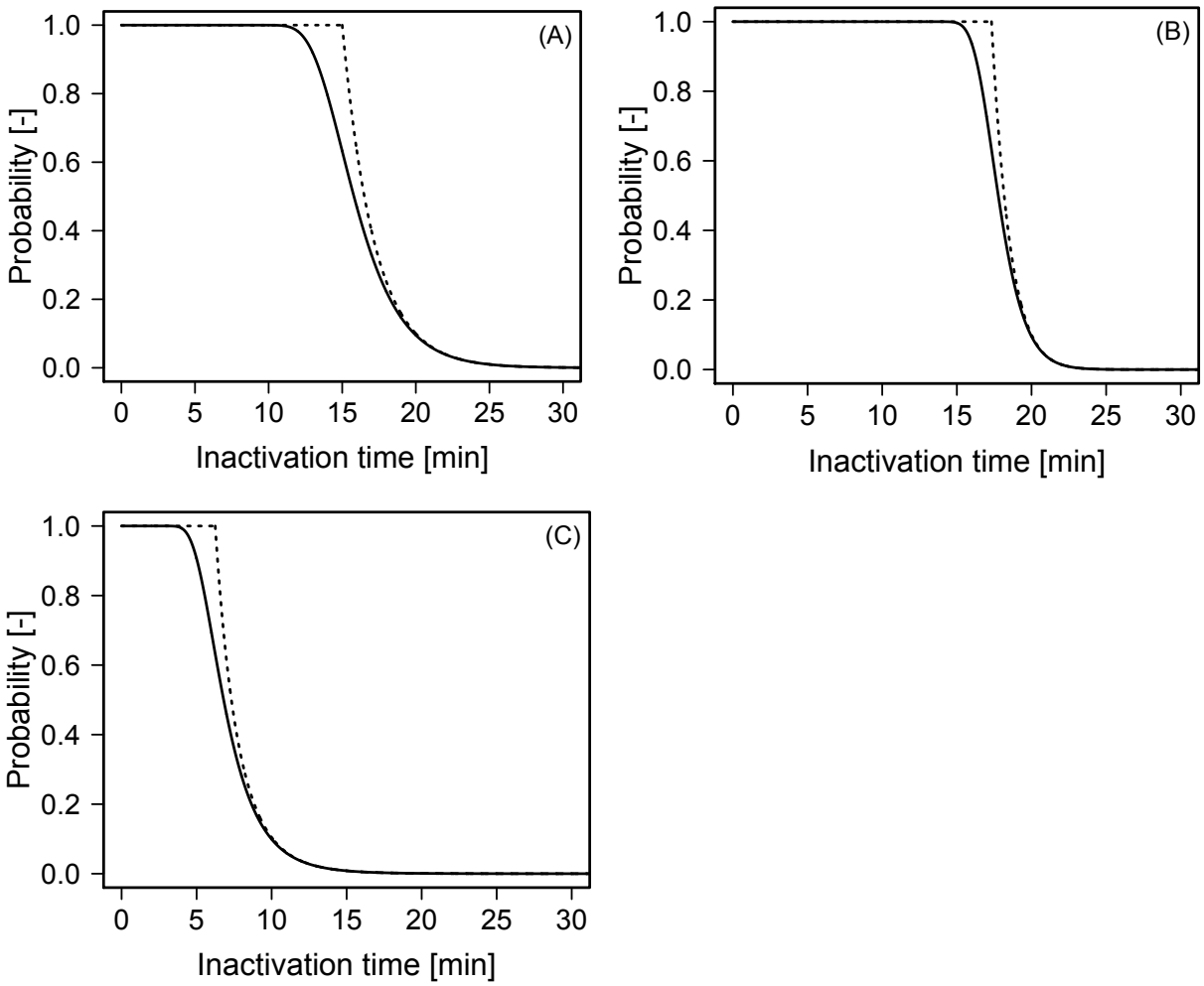


Fig. 3-6. Probability of a population containing survivors when $N_0 = 10^3$ cells under inactivation following a linear (A) (b = 0.2×log10, m = 1), downward (B) (b =0.01×log10, m=2), and upward curvature (C) (b = 1×log10, m = 0.6) model. Solid and dotted lines show probability of a population containing survivors calculated by probabilistic approach with individual cell heterogeneity and initial cell number (Eq. (3-11)) and inactivation kinetics model (Eq. (3-12)).

Table. 3-1. Comparison of probability of a population containing survivors between inactivation kinetic calculation (Eq. (3-12)) and stochastic calculation with variability in individual cell inactivation time and initial cell number (Eq. (3-11))

Kinetic	Stochastic	Percent difference
0.9	0.59	34.1
0.7	0.50	28.1
0.5	0.39	21.3
0.3	0.26	13.6
10^{-1}	0.95×10^{-1}	4.8
10^{-2}	0.995×10^{-2}	5×10^{-1}
10^{-3}	0.9995×10^{-3}	5×10^{-2}
10^{-4}	0.99995×10^{-4}	5×10^{-3}

3.3. Results and discussion

In the present study, we calculated the stochastic inactivation process of a bacterial population in two ways. In the first approach, the stochastic process calculated the time required for a specific decrease in the number of cells using the individual cell heterogeneity (Eq. (3-5)). Using this approach, we described the time required for a specific decrease in the number of cells as a probability distribution (Fig. 3-2). In addition, we calculated the probability of a population containing survivors and compared it with the *D*-value calculation (Fig. 3-3). Although there is an obvious difference between the stochastic and *D*-value calculations, this difference decreases as the probability of a population containing survivors becomes lower (Fig. 3-3). The second approach was to calculate the number of survivors using the individual cell heterogeneity and initial cell number variability. We described the number of survival cells as a Poisson distribution over time (Eq. (3-10)) (Fig. 3-5). Further, we compared the probability of a population containing survivors calculated from the stochastic approach with that given by the inactivation kinetics model (Fig. 3-6) and calculated the difference in the probabilities (Table 3-1). Although there are some differences

between the probabilistic approach and the kinetic method, the difference is less than 5% when the probability of a population containing survivors is below 0.1. Thus, the inactivation kinetics model is sufficient for calculating the probability of a population containing survivors at survival probabilities below 0.1. In contrast, the manually determined *D*-value model cannot properly calculate the probability of a population containing survivors when the inactivation kinetics model is not linear (Fig. 3-7). Thus, the *D*-value can over- or underestimate the probability of a population containing survivors. Instead of the *D*-value approach, a kinetics-based approach should be used in this case. In conclusion, we can use the kinetics approach to calculate the approximate probability of a population containing survivors at probabilities below 0.1.

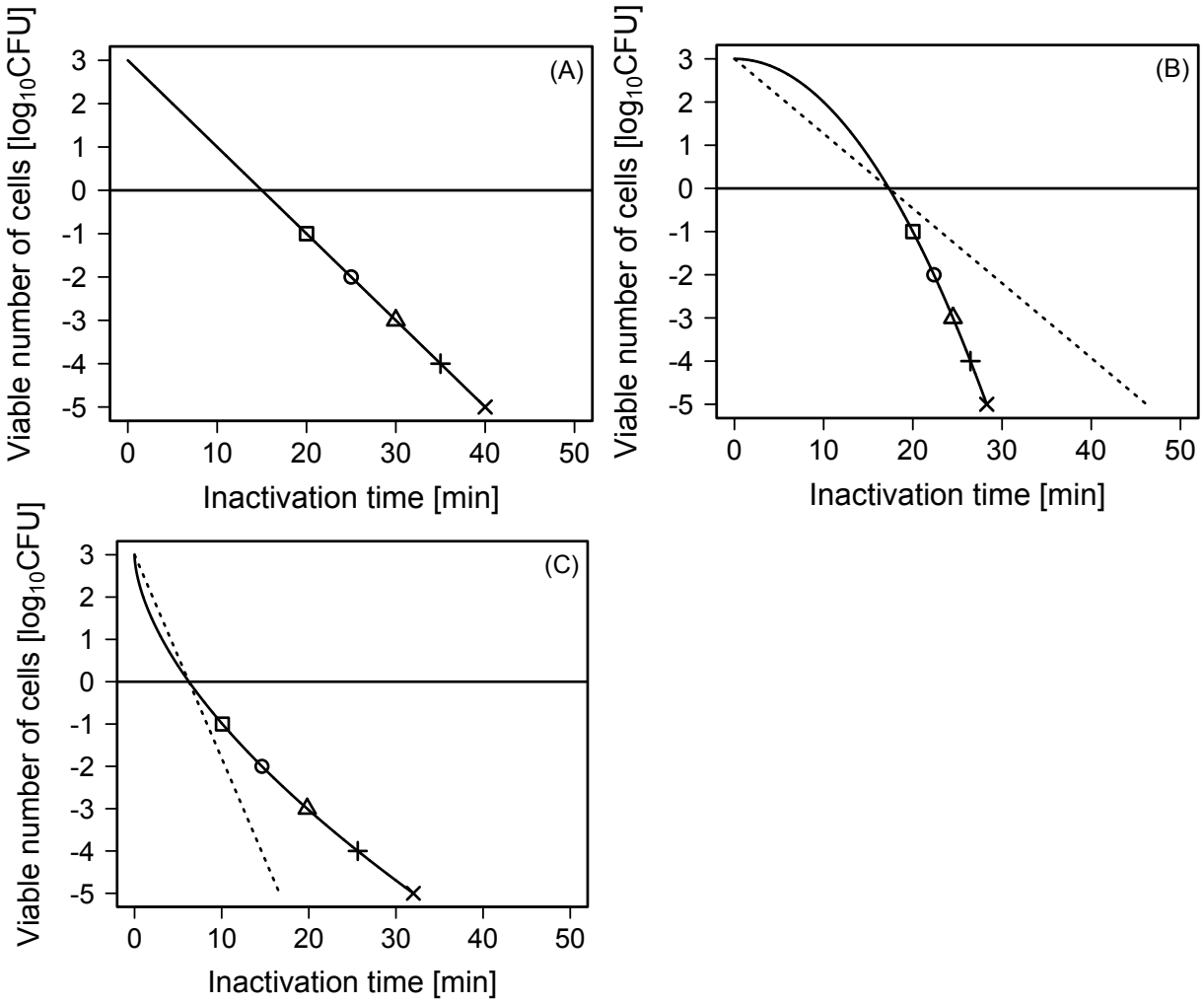


Fig. 3-7. Inactivation kinetics models and probability of a population containing survivors using inactivation kinetics model (b = 0.2×log10, m = 1) with downward concavity (b = 0.01×log10, m = 2) and upward concavity (b = 1×log10, m = 0.6) when $N_0 = 10^3$. The points $P_{kinetic}(t) = 10^{-1}$ (10% probability of survival), 10^{-2}, 10^{-3}, 10^{-4}, and 10^{-5} are indicated by a square, circle, triangle, plus, and cross, respectively. Dotted lines show an example of log-linear approximation.

The stochastic calculation of the time required for a specific decrease in the number of cells uses the convolution of the exponential distributions (Eq. (3-5)). Using this convolution result allowed a range of bacterial inactivation to be described, rather than simply giving the average (Fig. 3-2). The inactivation timing of individual cells was described by an exponential distribution (Eq. (3-3)). We revealed how individual cell inactivation affects variability in the inactivation behavior of the bacterial population. Our stochastic formula indicates that the variability in the bacterial inactivation process is universally calculated from the inactivation kinetics, regardless of the stress environment or bacterial strain. Thus, our calculation can explain general inactivation behavior. Our results provide the basis for computer simulations including individual cell heterogeneity.

We calculated the probability of a population containing survivors with variability in individual cell inactivation times and initial cell numbers, rather than using *D*-value calculations. We found that the inactivation curve provides an alternative method of calculating the probability of a population containing survivors. Our calculations indicate that the *D*-value is only suitable for linear models (Fig. 3-7). However, the *D*-value is not sufficient for estimating the probability of a population containing survivors, because the probability of a population containing survivors with respect to time exhibits some curvature (Fig. 3-7). Our stochastic approach calculates the probability of a population containing survivors considering the curvature of the inactivation kinetics, avoiding the need for manually determining the *D*-value (Peleg, 2006). Thus, our method gives a more appropriate inactivation time than the *D*-value approach. Optimum inactivation treatment improves food quality and requires less processing, such as for minimally processed foods.

When the inactivation kinetics are plotted in terms of the survivors with respect to time, the variability in bacterial behavior can be considered from two aspects. The first is the variability in the number of survivors (Aguirre et al., 2009; 2011; Koyama et al., 2017b; Rodriguez et al., 2016), which is shown on the y-axis of the survivors vs. time model. If we

assume that the cells initially follow a Poisson distribution, then the number of survivors can be theoretically described by a Poisson distribution (Aguirre et al., 2009; Koyama et al., 2017b; Kulkarni, 2016). The second aspect is the variability in the time required for a given decrease in the number of cells (Aspridou and Koutsoumanis, 2015; Koyama et al., 2017a), which is shown on the x-axis of the survivors vs. time model. Our stochastic theory is able to describe both types of variability (Eqs. (3-5) and (3-10)). Thus, variability in bacterial behavior should be clearly divided into the variability in the number of cells and the variability in the time required for a given decrease in the number of cells. Applying the variability in individual cells to an exposure assessment, the variability in both the x-axis and y-axis of the survivors vs. time model will play an important role, as it is vital to determine the probability of the number of survivors with respect to the elapsed time. Understanding the effect of individual cell heterogeneity on bacterial behavior would provide a more realistic estimation of bacterial survivors, rather than a worst-case scenario.

As a representative inactivation process, we cited a study on the inactivation of *Salmonella enterica* ser. Agona populations in a low-pH environment (Aspridou and Koutsoumanis, 2015). To examine the variability in the inactivation behavior, the *Salmonella enterica* population was inactivated 8–10 times in acidified tryptone soy broth (pH 3.5) with lactic acid. We illustrate the results of the observed *Salmonella* inactivation and our stochastic inactivation calculation with variability in the number of survivors given by a Poisson distribution (Eq. (3-10)) in Fig. 3-8. As the number of survivors decreases, the variability in the number of survivor increases on the log-scale. With time, the variability in the time required for a specific decrease in the number of cells increases. The *Salmonella* inactivation behavior and our stochastic inactivation calculation exhibit the same trend. One of the reasons for the stochastic inactivation process behind the inactivation trial can be explained by our theory. There are numerous food processing variables, such as heat, desiccation, high pressure, and ultraviolet light. The individual cell inactivation process

should be studied in each environment. In the case where the inactivation of individual cells is independent of other cells, our theory could be applied to describe the bacterial inactivation behavior.

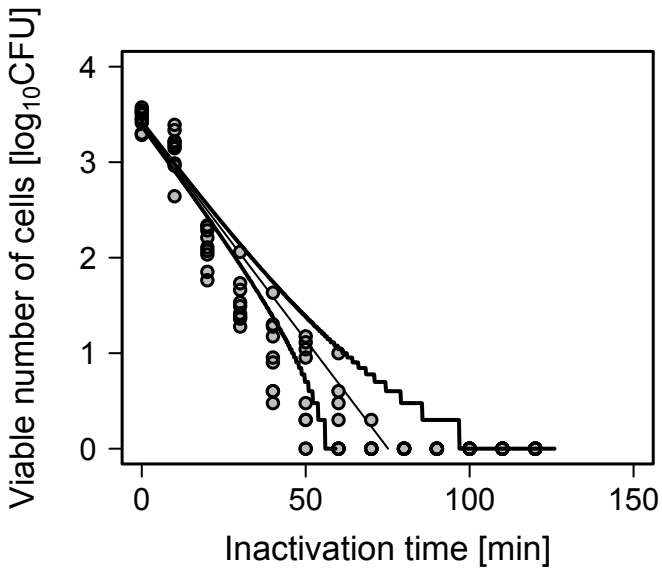


Fig. 3-8. Comparison between observed and theoretically calculated inactivation of *Salmonella enterica* ser. Agona populations with a mean initial level of $N_0 = 2511$ CFU/ml. Solid line shows inactivation kinetics. Bold solid line shows 0.005 and 0.995 quantiles of Poisson distribution with mean value $N(t) = N_0 e^{-bt^m}$. Experimental data and parameters of log-linear model (b = 0.104, m = 1) taken from Aspridou and Koutsoumanis (2015).

In the present study, we focused on stochastic bacterial inactivation behavior with bacterial states of survival or death. We assumed that there was no activation/inactivation of spore forming bacteria and no injury/recovery. In a realistic model, these states should be considered (Peleg, 2016). Our calculations have the limitation that the kinetics model does not provide detailed information about the bacterial state. To model bacterial inactivation behavior with a stochastic process, Peleg's inactivation model would be useful, although some method of detecting the differences between cell states should be developed (Corradini et al., 2010a; 2010b; Horowitz et al., 2009; Peleg, 2016).

The stochastic theory proposed in this study enables us to discuss the variability in the time required for a specific reduction in the number of cells and the probability of a population containing survivors, which has previously been evaluated by the *D*-value. We have previously developed a method for investigating the probability of a population containing survivors through 96 repetitions of bacterial inactivation (Koyama et al., 2017a). In future work, this bacterial inactivation experiment should be conducted to validate the model proposed in the present study. To analyze the randomness of the inactivation behavior in more detail, computer simulations will be needed in addition to the stochastic theory. Computer simulations based on the stochastic expressions developed in this study would provide an effective and powerful means of determining the variability trend of the bacterial inactivation behavior, as computer simulations can visualize the inactivation behavior of individual cells. Furthermore, our stochastic analysis may be applicable to bacterial growth, because the growth behavior of bacteria exhibits an exponential phase (Baranyi and Roberts, 1995). Thus, variability in the growth behavior could be calculated using our stochastic formulation. The stochastic theory presented in this study will enable a reinterpretation of bacterial behavior, which has long been described by changes in the average number of bacterial cells. Furthermore, the mathematical description of variability in bacterial inactivation represents a basic step toward a realistic risk assessment of bacterial survivors.

Chapter 4

Summary

In this study, we constructed a stochastic bacterial inactivation model using computer simulations and mathematical modeling. Chapter 2 presented an approach for estimating the time-to-inactivation and death probability of bacterial populations under the twin considerations of individual cell heterogeneity and the initial number of cells. Our simulation results showed that the time-to-inactivation significantly depends on the form of the kinetics curve and the initial number of cells. For example, with increases in the initial number of cells, the variance in the time-to-inactivation of log-linear, concave downward, and concave upward curves remains constant, decreases, and increases, respectively. A contour plot of the death probability was successfully generated via our computer simulation approach without using *D*-value estimation. Further, the death probability calculated using our stochastic approach was found to be almost the same as that obtained using inactivation kinetics. We validated the simulation results using data from the literature for the acid inactivation of *Salmonella* populations. The results of this study indicate that the inactivation curve can replace *D*-value extrapolation for estimating the death probability of bacterial populations. The proposed approach enables us to discuss the death probability of the bacterial population based on probability theory, instead of the traditional method of extrapolation applied to deterministic approaches. Our stochastic simulation for the death probability of bacterial populations can help to estimate the risk of bacterial survivors without recourse to the *D*-value concept.

In chapter 3, stochastic inactivation models were used in place of the conventional *D*-value to describe the probability of a population containing survivors. As representative bacterial inactivation normally follows a log-linear or log-Weibull model, we calculated the time required for a specific decrease in the number of cells and the number of surviving cells

as a probability distribution using the stochastic inactivation of individual cells in a population. We compared the probability of a population containing survivors calculated via the *D*-value, an inactivation kinetics model, and the stochastic formula. The stochastic calculation can be approximately estimated via a kinetics curvature model with less than 5% difference once the probability of a population containing survivors falls below 0.1. This stochastic formula indicates that the *D*-value model would over- or underestimate the probability of a population containing survivors when applied to inactivation kinetics that are not linear. The results presented in this study show that stochastic analysis using mathematical models accounting for variability in the individual cell inactivation time and initial cell number leads to a realistic and probabilistic estimation of bacterial inactivation. The proposed stochastic formulation enables an appropriate probability of a population containing survivors to be determined as an alternative to the conventional *D*-value method. The stochastic theory presented in this study permits a reinterpretation of bacterial behavior, which has long been described by changes in the average number of bacterial cells.

Our stochastic model and calculations describe the basic concept of stochastic inactivation of bacterial populations, which has previously been discussed in a deterministic manner. Our approach provides a valuable contribution to risk assessment frameworks, which need to treat the number of survivors and death probability of bacterial populations as probability distributions.

References

Aguirre, J.S., Pin, C., Rodriguez, M.R., Garcia de Fernando, G.D., 2009. Analysis of the variability in the number of viable bacteria after mild heat treatment of food. Appl. Environ. Microbiol. 75, 6992–6997. doi:10.1128/AEM.00452-09

Aguirre, J.S., Rodríguez, M.R., García de Fernando, G.D., 2011. Effects of electron beam irradiation on the variability in survivor number and duration of lag phase of four food-borne organisms. Int. J. Food Microbiol. 149, 236–246. doi:10.1016/j.ijfoodmicro.2011.07.003

Akkouchi, M., 2008. On the convolution of exponential distributions. J. Chungcheong Math. Soc. 21, 501–510.

Aspridou, Z., Koutsoumanis, K.P., 2015. Individual cell heterogeneity as variability source in population dynamics of microbial inactivation. Food Microbiol. 45, 216–221. doi:10.1016/j.fm.2014.04.008

Baranyi, J., Pin, C., 2001. A parallel study on bacterial growth and inactivation. J. Theor. Biol. 210, 327–336.

Baranyi, J., 2002. Stochastic modelling of bacterial lag phase. Int. J. Food Microbiol. 73, 203–206. doi:10.1016/S0168-1605(01)00650-X

Baranyi, J., Roberts, T.A., 1995. Mathematics of predictive food microbiology. Int. J. Food Microbiol. 26, 199–218.

Beuchat, L.R., Komitopoulou, E., Beckers, H., Betts, R.P., Bourdichon, F., Fanning, S., Joosten, H.M., Kuile, Ter, B.H., 2013. Low–Water Activity Foods: Increased Concern as Vehicles of Foodborne Pathogens. J. Food Prot. 76, 150–172. doi:10.4315/0362-028X.JFP-12-211

Brown, M., Stringer, M., 2002. Microbiological risk assessment in food processing. Woodhead Publishing, Cambridge, England.

Codex Alimentarius Commission, 2009. Principles and guidelines for the conduct of microbiological risk management (MRM). (CAC/GL 63-2007).

Corradini, M.G., Normand, M.D., Eisenberg, M., Peleg, M., 2010a. Evaluation of a Stochastic Inactivation Model for Heat-Activated Spores of *Bacillus* spp. Appl. Environ. Microbiol. 76, 4402–4412. doi:10.1128/AEM.02976-09

Corradini, M.G., Normand, M.D., Peleg, M., 2010b. Stochastic and Deterministic Model of Microbial Heat Inactivation. Journal of Food Science 75, R59–R70. doi:10.1111/j.1750-3841.2009.01494.x

Delignette-Muller, M.L., Rosso, L., 2000. Biological variability and exposure assessment. Int. J. Food Microbiol. 58, 203–212. doi:10.1016/s0168-1605(00)00274-9

El-Shaarawi, A.H., Esterby, S.R., Dutka, B.J., 1981. Bacterial density in water determined by Poisson or negative binomial distributions. Appl. Environ. Microbiol. 41, 107–116.

FAO/WHO, 2008. Exposure Assessment of Microbiological Hazards in Food. World Health Organization. Microbiological risk assessment series No. 7.

Fernández-Sestelo, A., de Saá, R.S., Pérez-Lamela, C., Torrado-Agrasar, A., Rúa, M.L., Pastrana-Castro, L., 2013. Overall quality properties in pressurized kiwi purée: Microbial, physicochemical, nutritive and sensory tests during refrigerated storage. Innovative Food Science & Emerging Technologies 20, 64–72. doi:10.1016/j.ifset.2013.06.009

Francois, K., Devlieghere, F., Smet, K., Standaert, A.R., Geeraerd, A.H., Van Impe, J.F., Debevere, J., 2005. Modelling the individual cell lag phase: effect of temperature and pH on the individual cell lag distribution of *Listeria monocytogenes*. Int. J. Food Microbiol. 100, 41–53. doi:10.1016/j.ijfoodmicro.2004.10.032

Haas, C.N., Rose, J.B., Gerba, C.P., 1999. Quantitative microbial risk assessment. John Wiley & Sons, New York, USA.

Hara-Kudo, Y., Takatori, K., 2011. Contamination level and ingestion dose of foodborne pathogens associated with infections. Epidemiol. Infect. 139, 1505–1510. doi:10.1017/S095026881000292X

Horowitz, J., Normand, M.D., Corradini, M.G., Peleg, M., 2009. Probabilistic Model of Microbial Cell Growth, Division, and Mortality. Appl. Environ. Microbiol. 76, 230–242. doi:10.1128/AEM.01527-09

Koseki, S., Matsubara, M., Yamamoto, K., 2009. Prediction of a required log reduction with probability for *Enterobacter sakazakii* during high-pressure processing, using a survival/death interface model. Appl. Environ. Microbiol. 75, 1885–1891. doi:10.1128/AEM.02283-08

Koutsoumanis, K.P., Aspridou, Z., 2017. Individual cell heterogeneity in Predictive Food Microbiology: Challenges in predicting a “noisy” world. Int. J. Food Microbiol. 240, 3–10. doi:10.1016/j.ijfoodmicro.2016.06.021

Koyama, K., Hokunan, H., Hasegawa, M., Kawamura, S., Koseki, S., 2017a. Estimation of the probability of bacterial population survival: Development of a probability model to describe the variability in time to inactivation of *Salmonella enterica*. Food Microbiol. 68, 121–128. doi:10.1016/j.fm.2017.07.007

Koyama, K., Hokunan, H., Hasegawa, M., Kawamura, S., Koseki, S., 2017b. Modeling Stochastic Variability in the Numbers of Surviving *Salmonella enterica*, Enterohemorrhagic *Escherichia coli*, and *Listeria monocytogenes* Cells at the Single-Cell Level in a Desiccated Environment. Appl. Environ. Microbiol. 83, e02974–16. doi:10.1128/AEM.02974-16

Koyama, K., Hokunan, H., Hasegawa, M., Kawamura, S., Koseki, S., 2016. Do bacterial cell numbers follow a theoretical Poisson distribution? Comparison of experimentally obtained numbers of single cells with random number generation via computer simulation. Food Microbiol. 60, 49–53.

Kulkarni, V.G., 2016. Modeling and Analysis of Stochastic Systems, Third Edition. CRC Press, London, United Kingdom.

McClure, P.J., de W Blackburn, C., Cole, M.B., Curtis, P.S., Jones, J.E., Legan, J.D., Ogden, I.D., Peck, M.W., Roberts, T.A., Sutherland, J.P., Walker, S.J., 1994. Modelling the growth, survival and death of microorganisms in foods: the UK Food Micromodel approach 23, 265–275. doi:10.1016/0168-1605(94)90156-2

McMeekin, T.A., Olley, J., Ratkowsky, D.A., Ross, T., 2002. Predictive microbiology: towards the interface and beyond. International Journal of Food Microbiology 73, 395–407. doi:10.1016/S0168-1605(01)00663-8

Membré, J.M., Amézquita, A., Bassett, J., Giavedoni, P., Blackburn, C. de W., Gorris, L.G.M., 2006. A probabilistic modeling approach in thermal inactivation: estimation of postprocess *Bacillus cereus* spore prevalence and concentration. J. Food Prot. 69, 118–129.

Ministry of Health, Labor and Welfare, 2017, https://www.mhlw.go.jp/file/05-Shingikai-11121000-Iyakushokuhinkyoku-Soumuka/0000197210.pdf

Nauta, M.J., 2002. Modelling bacterial growth in quantitative microbiological risk assessment: Is it possible? Int. J. Food Microbiol. 73, 297–304.

Nauta, M.J., 2000. Separation of uncertainty and variability in quantitative microbial risk assessment models. Int. J. Food Microbiol. 57, 9–18. doi:10.1016/s0168-1605(00)00225-7

Peleg, M., 2006. Advanced Quantitative Microbiology for Foods and Biosystems. CRC Press, Boca Raton, FL.

Peleg, M., Cole, M.B., 1998. Reinterpretation of Microbial Survival Curves. Crit. Rev. Food Sci. Nutr. 38, 353–380. doi:10.1080/10408699891274246

Peleg, M., Normand, M.D., 2004. Calculating microbial survival parameters and predicting survival curves from non-isothermal inactivation data. Crit. Rev. Food Sci. Nutr. 44, 409–418. doi:10.1080/10408690490489297

Peleg, M., 2016. Modeling Microbial Inactivation by Pulsed Electric Field, in: Miklavcic, D. (Ed.), Handbook of Electroporation. Springer International Publishing, Cham, pp. 1–18. doi:10.1007/978-3-319-26779-1_43-1

Rodriguez, M.R., Aguirre, J.S., Lianou, A., 2016. Analysis of the variability in microbial inactivation by acid treatments. LWT – Food Sci. Technol. 66, 369–377. doi:10.1016/j.lwt.2015.10.056

Ross, T., McMeekin, T.A., 1994. Predictive microbiology 23, 241–264. doi:10.1016/0168-1605(94)90155-4

Ross, T., McMeekin, T.A., 2003. Modeling microbial growth within food safety risk assessments. Risk Anal. 23, 179–197. doi:10.1111/1539-6924.00299

Schaffner, D.W., 2008. Microbial Risk Analysis of Foods. ASM Press, Washington, D.C.

Standaert, A.R., Geeraerd, A.H., Bernaerts, K., Francois, K., Devlieghere, F., Debevere, J., Van Impe, J.F., 2005. Obtaining single cells: Analysis and evaluation of an experimental protocol by means of a simulation model. Int. J. Food Microbiol. 100, 55–66.

Teunis, P.F.M., Kasuga, F., Fazil, A., Ogden, I.D., Rotariu, O., Strachan, N.J.C., 2010. Dose-response modeling of *Salmonella* using outbreak data. 144, 243–249. doi:10.1016/j.ijfoodmicro.2010.09.026

van Asselt, E.D., Zwietering, M.H., 2006. A systematic approach to determine global thermal inactivation parameters for various food pathogens. Int. J. Food Microbiol. 107, 73–82.

van Boekel, M.A.J.S., 2002. On the use of the Weibull model to describe thermal inactivation of microbial vegetative cells. Int. J. Food Microbiol. 74, 139–159.

Vervoort, L., Van der Plancken, I., Grauwet, T., Timmermans, R.A.H., Mastwijk, H.C., Matser, A.M., Hendrickx, M.E., Van Loey, A., 2011. Comparing equivalent thermal, high pressure and pulsed electric field processes for mild pasteurization of orange juice. Innovative Food Science & Emerging Technologies 12, 466–477. doi:10.1016/j.ifset.2011.06.003

Voysey, P.A., Brown, M., 2000. Microbiological risk assessment: a new approach to food safety control. Int. J. Food Microbiol. 58, 173–179. doi:10.1016/S0168-1605(00)00271-3

Who, 2017, Food safety, https://www.who.int/news-room/fact-sheets/detail/food-safety

Xiong, R., Xie, G., Edmondson, A.E., Sheard, M.A., 1999. A mathematical model for bacterial inactivation. Int. J. Food Microbiol. 46, 45–55.

Zwietering, M.H., 2002. Quantification of microbial quality and safety in minimally processed foods. Int. Dairy J 12, 263–271. doi:10.1016/s0958-6946(01)00156-x

Approaches for probabilistic evaluation in predictive microbiology: Interpretation of stochastic bacterial inactivation process at population and single-cell levels

March, 2019

Kento Koyama

Laboratory of Agricultural and Food Process Engineering
Division of Biosystems Sustainability
Graduate School of Agricultural Science, Hokkaido University
Kita-9, Nishi-9, Kita-ku, Sapporo, Hokkaido, Japan
Tel. and Fax.: +81-11-706-2558